Investigating Alternative Testing Techniques for Evaluating the Environmental Stress Cracking Resistance of Polyethylenes in Contact with Ageing Fluids

Investigating Alternative Testing Techniques for Evaluating the Environmental Stress Cracking Resistance of Polyethylenes in Contact with Ageing Fluids

By: William T.J. West, B.Eng.Biosci

A Thesis Submitted to the School of Graduate Studies in Partial Fulfillment of the Requirements for the Degree Master of Applied Science

Lay Abstract

Accelerated failure of stressed plastics can occur upon exposure to fluids through a phenomenon known as environmental stress cracking (ESC). The following research outlines the development of a novel testing technique to gauge a material's environmental stress cracking resistance (ESCR). Adaption of passive acoustics to an existing stress cracking test was unable to provide any indication of ESCR, however the use of active ultrasonics was able to show sample plasticization. A novel forced based measuring technique was found to uniquely map the failure progression of a sample undergoing ESC, providing valuable information for understanding the phenomenon. Additional testing was also completed on various environmental fluids to reveal biodiesel's ability to provoke ESC, an important observation.

Abstract

Environmental stress cracking (ESC) is a significant problem that has plagued the plastics industry since its discovery nearly 70 years ago. The accelerated brittle failure brought about when a stressed polymer comes in contact with an aggressive environment can happen suddenly with destructive results. Many classes of polymers are susceptible to this type of slow crack growth; however special emphasis has typically been placed on polyolefins due to their wide range of working environments, market dominance and their seemingly chemical resistance. Much research has been focused on formulating environmentally resistant materials, while the evaluation techniques for gauging environmental stress cracking resistance (ESCR) seem to have been left behind. This research focuses on developing a reliable testing technique for evaluating the ESCR of polyethylene resins.

Passive acoustic monitoring was adapted to an industrially accepted ESCR test in an attempt to hear polymer damage before it was visually apparent. It was discovered that the low energy released during the early stages of damage and excessive background noise masked passive signals, making this method of evaluation impractical. Alternatively, active ultrasonic monitoring through velocity and attenuation measurements was investigated to see if probing techniques could be used to detect structural damage. Active ultrasonic monitoring of static and tensile stressed samples were able to differentiate plasticization after ageing, however no indication of ESCR properties could be inferred.

A novel forced based monitoring system was developed in response to the acoustic testing techniques. Force monitoring was able to provide useful information regarding the failure cycle of ESC and the acquired profiles could describe a failure onset time. Several ageing environments were also tested with force monitoring and a traditional ESCR test to reveal the stress cracking ability of biodiesel, an important finding.

Acknowledgments

Over the past 24 months I have learned a tremendous amount, not just about polymers but critical problem solving skills and most importantly just how to be a better person. My supervisor, Dr. Michael Thompson, has proven to be an excellent role model and I owe a lot of what I have learned to his support and guidance.

I want to thank Imperial Oil and Ron Cooke for the supply of material and professional advice on polymer resins which made this research possible.

I would like to thank a good friend Brady Semple for the insightful talks we have had and the help he provided with LabVIEW coding and assistance with acquiring the excellent microscope images.

Finally I would like to thank my parents and friends whose continued support and words of encouragement have proven to be invaluable.

Table of Contents

Introduction and Background 1
Experimental Methods 11
Selected Materials 11
Polymers 11
Ageing Fluids 11
Ultrasonic Testing 12
Hardware 12
Software 12
Materials Testing 13
Differential Scanning Calorimetry 13
Tensile Testing 13
Microscopy 14
Environmental Stress Cracking Resistance Testing 14
Development of a Passive Acoustics Testing Method for the Evaluation of ESCR 15
Introduction 15
Testing Configurations & Results 15
Large Scale Tank 15
Single Heated Sample Testing – Mason Jar 18
Alternative Transducer Coupling Configurations 19
Small Scale Tank with Video Monitoring 21
Conclusions 23
Development of an Active Acoustics Testing Method for the Evaluation of ESCR 25
Introduction 25
Testing Configurations and Results 25
Conclusions 33
Development of a Force Based Measurement System for the Evaluation of ESCR 35
Introduction 35
Preliminary Work 38
Effects of Sample Length on Failure Time 40
Designed Equipment 43
Effects of Ageing Fluid on Sample Failure Time 46

Grade 1 46
Grade 7 51
Grade 4 54
Conclusions 55
Evaluation of Biodiesel as an Environmental Stress Cracking Agent 57
Introduction 57
Testing and Results 58
Conclusions 60
Final Conclusions 61
Recommendations for Future Work 62
References 64
Appendix A – Supplementary Figures 67

List of Figures

Figure 1: Bell Test equipment, with A) representing the notching device and B) showing 10 bent samples in ageing fluid [3]. 2
Figure 2: A) Dog bone sample configuration for NCTL Test with notch and mounting holes shown. B) Testing rack for inducing constant stress in the NCTL Test [4]. 3
Figure 3: Example of brittle fracture in polyethylene, showing smooth surface. Adapted from [16] 6
Figure 4: Scanning electron micrograph of medium density polyethylene after 30 hours in a constant load tensile test. Primary and secondary crazes are evident, showing stages of slow crack growth. Adapted from [18] 6
Figure 5: Depiction showing three main types of interlamellar interactions of semi-crystalline materials. a) Tie Molecules, b) Loose loops/Cilia, c) Entangled Loops. Adapted from [19] 7
Figure 6: Larger molecular weight polyethylenes have a larger fracture stress when tested under a fast fracture technique using liquid nitrogen. Adapted from [28] 9
Figure 7: Environment stress cracking resistance improves with lager lamellar surface area. Adapted from [31] 10
Figure 8: Initial Bell Test tank set-up with external VWR water bath highlighted. 16
Figure 9: Sensor mounting device. 17
Figure 10: Main acoustic signals obtained from the hybrid ASTM D1693 test. Low frequency dominant waveform is shown in (a), while high frequency dominant in (b). The top portion of each plot is the actual recorded signal; the bottom is the respective FFT. 18
Figure 11: Simplified Mason jar testing configuration. 19
Figure 12: Typical noise signal obtained from the simplified set-up. Actual signal is represented in the top plot, with the FFT shown below. 19
Figure 13: Alternative acoustic sensor mount for more direct detection of fracture evens during stress cracking tests. 20
Figure 14: Second generation Bell Test set-up constructed from rectangular plastic tank. Immersion heated, web-camera and addition lighting was used to improve failure detection. 21
Figure 15: ESCR Test used to identify possible sample derived acoustic activity. 22
Figure 16: Comparison of Grade 1 pre and post ageing in a 10% solution of Igepal and water. Extensive cracking after a short period of time (4 hours) is highlighted. 23
Figure 17: Comparison of relative mass changes for resin Grades 1, 2, 4, and 6 after ageing for 124 hr in solutions of Toluene (**Top**), 10% Igepal (**Middle**) and B100 biodiesel (**Bottom**). The relative standard error for the measurements was ± 0.02%. ● = Grade 1, ■ = Grade 2, ◢ = Grade 4, and ◆ = Grade 6. 27
Figure 18: Relative change in ultrasonic velocity for resin Grades 1, 2, 4, and 6 after exposure to either Toluene (**Top**), 10% Igepal (**Middle**) or B100 biodiesel (**Bottom**) after select periods of time. The relative standard error for the measurements was ± 0.02%. ● = Grade 1, ■ = Grade 2, ◢ = Grade 4, and ◆ = Grade 6. 29
Figure 19: A comparison of relative changes in ultrasonic velocity of HDPE resin samples during a tensile/relaxation test after ageing for 124 hours in specific environments. The symbols of the points corresponds to the environment, with ● = Virgin, ◢ = Toluene, ✕ = Igepal, and ■ = Biodiesel. Only one sample from each resin Grade was tested in the three environments. The relative standard error for the measurements was ± 0.01%. 31

Figure 20: Elastic Modulus of each Grade of polymer resin after ageing for 124 hours in specific contacting fluids. ■ = Virgin, ■ = Toluene, ■ = Igepal, and ■ = Biodiesel..... 33
Figure 21: Force response curves from the Plate Test ESCR evaluation technique. Figure adapted from [40]..... 36
Figure 22: Comparison of ESCR testing times for the Bell Tests and Plate Test. Figure adapted from [40]. 36
Figure 23: Visible stress cracks after an indentation test in a solution of 10% Igepal at 50°C. Figure Adapted from [41] 37
Figure 24: KISTLER force sensor with constrained polymer sample. 39
Figure 25: Force profiles obtained from KISTLER Sensor for Grade 1 resin aged in a 10% Igepal solution. 40
Figure 26: OMEGA sensor with mounted polymer sample. 41
Figure 27: Load cell signal conditioner. 41
Figure 28: Failure profiles for varying lengths of Grade 2 resin after ageing in a 50°C bath of 10% Igepal solution. 41
Figure 29: Re-run of varying sample length to determine optimal failure time. Fracture line is shown as the horizontal dashed red line. 42
Figure 30: Notching and bending device. A photo of the assembled unit is shown to the left with the male plunger highlighted whereas a cross-section is shown on the right with bent sample and razor blade in place. 44
Figure 31: Acrylic sample retaining device with fitted OMEGA sensor to read forces in a compressive manner. 45
Figure 32: Force profiling curves for Grade 1 resin aged in 100% and 10% Igepal, B100 biodiesel and air. Dashed vertical lines at 1.9 hr and 2.9 hr represent when a separate sample of Grade 1 was removed and imaged. Fracture line is shown as the horizontal dashed red line. Peak loadings never exceeded ~30 N. 46
Figure 33: Images of Grade 1 resin after ageing in a 10% solution of Igepal in water for 1.9 hr. (Images on left) and 2.9 hr. (Images on right). A) Sample apex B) Notch Tip C) Striation formation 48
Figure 34: Newly formed fracture surface of Grade 1 polymer after ageing in Air, Biodiesel and 10% Igepal. The notch tip is identified for each sample with a red arrow. The fracture surface naturally progresses width-wise across the sample, perpendicular to the notch 49
Figure 35: Grade 7 force profiling after ageing in 100% and 10% Igepal, B100 biodiesel and 50°C air. Fracture line is shown as the horizontal dashed red line 51
Figure 36: Notch tip of a G7 sample pre-ageing (A) and after aged in Biodiesel for 116 hr (B). 52
Figure 37: Grade 4 force profiling showing only, the initial relaxation and plateau region after 42 hours of ageing. Fracture line is shown as the horizontal dashed red line 54
Figure 38: Excellent example of environmental stress cracking occurring at the notch tip after an undefined period of ageing. A fresh notch (A) is compared against the aged sample (B). 55
Figure 39: Staining of the fracture area by biodiesel on a sample of Grade 1 polyethylene. 59
Figure 40: Alternative ESCR testing configuration where a compressed pipe could be submerged in a heated bath to monitor force loading. 63

List of Tables

Table 1: Summary of key material properties for all resins used in experimental work..... 11
Table 2: Average failure time of Grade 1 after exposure to varying environments. Error in failure time reflects the standard error of three trials..... 50
Table 3: Average failure onset time of Grade 1 after exposure to varying environments. Error in failure time reflects standard error of three trials..... 51
Table 4: Average failure time of Grade 7 after exposure to varying environments. Error in failure time reflects standard error of three trials..... 53
Table 5: Average failure onset time of Grade 7 after exposure to varying environments. Error in failure time reflects standard error of three trials..... 53
Table 6: Environmental stress cracking agents identified through use of the Bell Test. Table adapted from [6]..... 57
Table 7: Determined ESCR values for polyethylene resins aged in a solution of 10% biodiesel in water or 10% biodiesel in petroleum based diesel..... 60

Introduction and Background

Polyolefins are unquestionably prevalent in the modern world, with applications ranging from industrial piping networks to simple household recycling bins. The relatively inert nature of this polymer class, combined with a spectrum of possible mechanical properties makes them a common material for long lifespan products. The service life of polyethylenes can usually range from years to decades before intervention or replacement is needed. Unfortunately, this is not always the case, as premature failure caused by environmental factors is well-documented, including a famous case occurring for the Western Electric Company.

In the late 1940's Western Electric was beginning to use Low Density Polyethylene (LDPE) as a jacketing material for their wiring, to replace a previously used class of elastomer. Shortly after final installation of the jacket, it was noticed that the LDPE was cracking prematurely. Bell Laboratories, a research division of Western Electric, investigated this issue and discovered that the soapy lubricant used to make the jacket installation easier was causing the cracks to form [1]. Examples of accelerated failure in polyolefins and even more so, glassy polymers, were beginning to be seen world-wide and the phenomenon being witnessed was characterized as Environmental Stress Cracking (ESC) [2].

The realization that polyethylenes could fail unexpectedly in the field led to manufacturers and users of the material to question their safety and effectiveness at withstanding harsh environmental conditions. To try and quantify the potential lifespan of polyethylenes, Bell Laboratories developed an environmental stress cracking resistance (ESCR) test based on the conditions under which they witnessed jackets failing. The resulting test, designated ASTM D1693 and commonly known as the Bell Test, involves the submersion of bent and razor-notched samples of polyethylene in a heated solution of an environmental stress cracking agent, typically Igepal CO630 [2, 3]. To perform a test, ten samples of a given polyethylene are notched longitudinally on one face with a notching jig, then bent and secured in a brass u-channel which is placed in a glass test tube. The stress cracking agent is then added to the test

tube at a concentration of either 10%/100% and aged at 50°C (Condition A & B) or 100% at 100°C (Condition C) to promote rapid failure and relatively short test times.[1] An illustration of the notching jig and test tube containing notched samples can be seen in Figure 1 below.

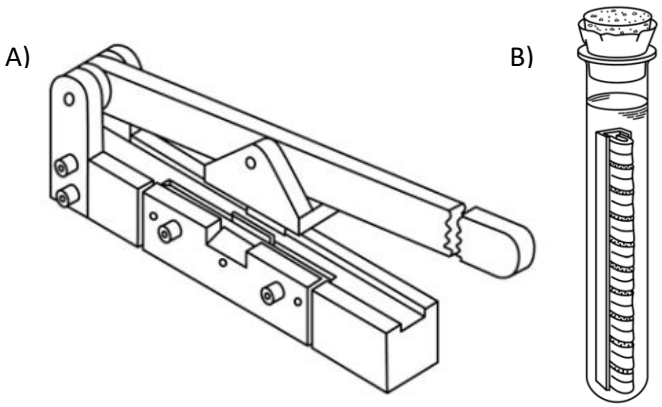

***Figure 1**: Bell Test equipment, with A) representing the notching device and B) showing 10 bent samples in ageing fluid [3].*

The ESCR value of a polymer resin from this test is quoted in hours, which is a measure of how long it took for 50% of the mounted samples (F_{50}) to fail upon visual inspection. The simplicity of the Bell Test has allowed it to become one of the most widely used methods for evaluating ESCR, however test inconsistencies (failure detection method/non-constant applied stress) and long testing times (>3000 hrs) have brought about the need for an alternative testing method that improves on these limitations.

The development of geomembranes has been a major driver towards the creation of an improved ESCR test since they are subjected to arguably the harshest environmental conditions, as liners to landfills and liquid hazardous waste sites. In an attempt reduce failure times, ASTM D5397, known as the notched constant tensile load test (NCTL Test), was developed and follows a similar approach to a mechanical tensile test [4]. As shown in Figure 2, dog-bone cut samples are razor notched horizontally on one face and submerged in a 50°C heated bath of a 10% Igepal and water solution.

[1] Testing conditions vary with sample thickness (t). Condition A, t = 3.00 – 3.30 mm, Condition B, t = 1.84 – 1.97 mm, and Condition C, t = 1.84 – 1.97 mm.

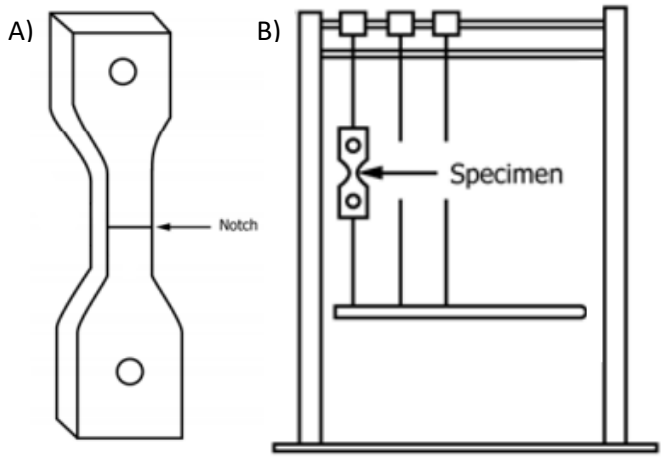

***Figure 2**: A) Dog bone sample configuration for NCTL Test with notch and mounting holes shown. B) Testing rack for inducing constant stress in the NCTL Test [4].*

This ASTM standard calls for a progressive increase of applied stress to each sample, ranging from 20 – 60% of the yield stress, which can be implemented through a weighted lever system. Unlike the Bell Test, failure time is recorded for each individual sample with a timed clock operated though the lever system. After multiple tests have been completed, a plot can be created depicting the applied stress vs. failure time. It is often noted that this procedure for determining the ESCR can still be rather lengthy due to number of tests required to generate the plot. To try and condense the analysis of ESCR, Hsuan and Koerner developed an extension to this ASTM, known as the Single Point – Notched Constant Load Test, where the load is fixed at 30% of the yield stress, as this has been determined to produce short failure times with brittle fracture [5]. The final ESCR value is quoted as being the mean failure time from five samples tested under the same conditions.

Environmental stress cracking resistance test methods have also been developed that are tailored to polyethylene pipes and resins, such as ASTM F1473, commonly known as the Pennsylvania Notch Test (PENT). The PENT is structured similarly to the NCTL Test, where a sample is tested in tension under a constant stress (2.4 MPa), however sample geometry differs as a rectangular profile is used opposed to the dog-bone shape and *three* coplanar notches are present to increase stress concentration [6]. Samples are aged in an air bath held at a constant temperature of 80°C and failure is detected though a timed

switch using the same principle as the NCTL Test. This test focuses on observing the progression of slow crack growth, a proposed mechanism behind environment stress cracking, however the absence of a stress cracking agent leads to long testing times. A European equivalent to this test, called the Full Notch Creep Test (ISO 16770) utilizes rectangular profile samples, razor-notched on all *four* faces with submersion in a heated environmental bath under tensile load to remedy the extended times associated with ASTM F1473 [7].

A relative ranking of how well different polyethylene resins perform against each other can be created through the previously mentioned tests. However, these methods have been known to contradict each other or worse, fail to reasonably predict polymer performance in industrial applications. A common discrepancy arises between constant strain (Bell Test) and constant load (NCTL Test, PENT) tests as they fail to consider the influence of mechanical properties on a material's performance. During the bending procedure of the Bell Test, the stiffness inherent to high density polyethylene (HDPE) samples subjects them to stresses close to, or beyond their yield point [8]. The same bending action performed on a low density polyethylene (LDPE) sample imposes a much smaller stress, which leads to a common result of HDPE failing sooner than LDPE. The complete opposite is typically seen in constant load tests, where LDPE is stressed closer to its yield point and is seen to fail quicker than HDPE [8].

Considering the limitations of the previously discussed mechanical based tests, the following study focuses on the environmental stress cracking resistance of high density polyethylene with specific objectives as outlined below.

- Design and implementation of an alternative test to evaluate the ESCR of polyethylenes.
- Evaluation of the possibility of biodiesel being an environmental stress cracking agent.
- Observe the crack formation and propagation within various high density polyethylene resins subjected to different environmental agents.

Literature Review

It has been estimated 15-40% of all plastic component failures can be traced to a phenomenon known as environmental stress cracking [9, 10]. Wright provided an excellent overview of ESC, describing it as; *"The premature initiation of cracking and embrittlement of a plastic due to the simultaneous action of stress and strain and contact with specific fluids" [9].* Environmental stress cracking itself is a physical phenomenon, meaning the fluids in contact with a stressed polymer **do not** chemically alter the polymer structure; embrittlement occurs due to the physical interaction of the environment with polymer chains [11].

Documentation of ESC type failures began approximately 75 years ago, with premature cracking of LLDPE wire jacketing for the Western Electric company serving as a signature event. The work by Bell Laboratories to describe this unusual phenomenon can be considered the beginning for understanding the workings of ESC as material properties influencing cracking resistance had been identified and a novel testing system for ESCR evaluation had been created (ASTM D1694) [2]. Since the identification of environmental accelerated failure, a push has been made to try and fully understand its mechanisms as a range of polymers classes have been found susceptible [12-15]. Even though the majority of work performed on studying ESC has involved polyethylenes, many unanswered questions still remain and the following Chapter describes the current understanding of ESC as it pertains this material.

Early work done at Bell Laboratories characterized ESC as a type of slow crack growth (SCG), which results in brittle facture of the material [1]. Brittle facture from a macroscopic perspective, shown in Figure 3, appears as a clean break with a characteristic smooth surface lacking large fibrils; fibrils being more of an indicator of ductile failure.

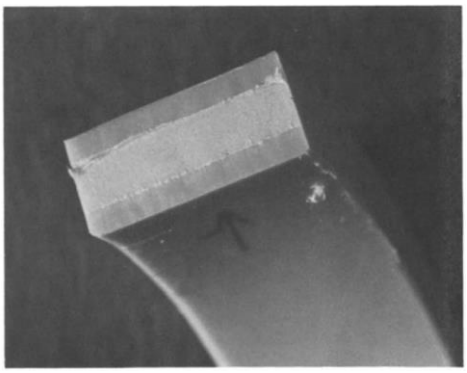

Figure 3: Example of brittle fracture in polyethylene, showing smooth surface. Adapted from [16]

Slow crack growth typically develops over a long period of time when a material is under low stresses and craze formation gives way to a crack. Deblieck et al. [17] explain that a craze initiates when a section of the material concentrates stresses at a pre-existing defect such as a nick or a scratch. These concentrated stresses then result in a disturbance of the polymeric microstructure and a void will open in the interlamellar amorphous region. Over time, Deblieck further explains that the void will propagate in a direction perpendicular to the highest principal stress, leaving behind the formation of a crack [17]. Eventually, the craze/crack will grow so large that a steady, small stress will cause complete brittle failure. Lustiger and Corneliussen were able to show an excellent representation of the SCG process by performing a constant tensile load test on a notched sample of medium density polyethylene [18]. The scanning electron micrograph shown in Figure 4 depicts a notched sample after 30 hr of testing, where *multiple* crazes are apparent.

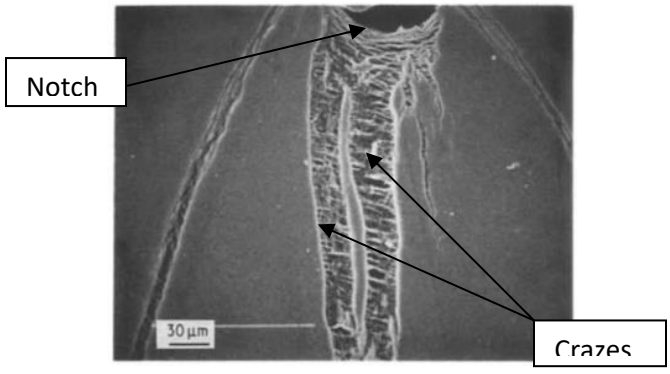

Figure 4: Scanning electron micrograph of medium density polyethylene after 30 hours in a constant load tensile test. Primary and secondary crazes are evident, showing stages of slow crack growth. Adapted from [18]

A more detailed view of SCG in polyolefins can be examined by focusing on the interlamellar amorphous region. This region is generally agreed upon as being responsible for the mechanical strength and crack resistant properties of semi-crystalline materials [19]. Three main classes of crystalline/amorphous interactions have been identified with the most important being tie molecules (TMs). Tie molecules are large molecular weight polymer chains that are distinct in physically linking crystal lamella together by spanning the intermediate amorphous region. Ciliated loops also exist, which, when entangled, link lamella together, but are not considered as strong as TMs. The weakest interaction involves simple chain entanglements arising from loose loops or cilia occurring in the amorphous region. Seguela provided a good visual depiction of these interactions which can be seen in Figure 5 [19].

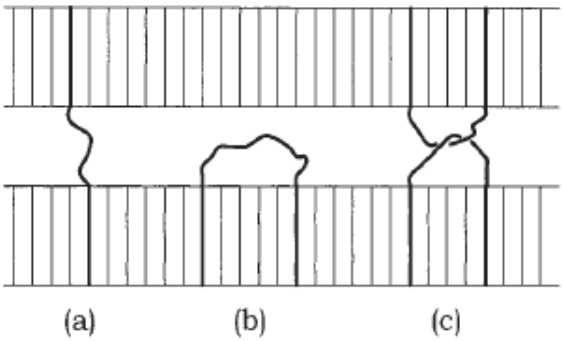

Figure 5: Depiction showing three main types of interlamellar interactions of semi-crystalline materials. a) Tie Molecules, b) Loose loops/Cilia, c) Entangled Loops. Adapted from [19]

Researchers have used these interlamellar interactions to describe the progression of SCG in a semi-crystalline polymer. It is agreed that under low stresses, chain entanglements are able to relax, leaving only TM's and linked loops binding crystalline regions together. Over time, TM's begin to stretch, forming a craze and eventually they **slip or break** from their respective lamella releasing energy to form a crack and ultimately a fracture [20]. The SCG mechanism can mostly describe ESC, the main distinction being ESC occurs at an accelerated pace.

The accelerated cracking phenomenon seen in ESC has been examined quite extensively in polyolefins and it has been established that detergents are the most intensive stress cracking agents.

Igepal CO630 has historically been identified as an excellent environment for testing ESCR due to its ability to provide rapid failure times over a range of concentrations and its low risk when handled or exposed to elevated temperatures. This environment was used throughout DeCoste et al's signature tests and has since become the standardized environment for evaluation of ESC in polyethylenes [2]. Traditionally either a full strength or 10% aqueous solution of Igepal would be used for testing ESCR, however peak potency has been identified at approximately 50%, with decreased activity at both extremes of 0.01% and 100% [21, 22]. Despite the lower potency of Igepal at decreased concentrations, its presence provokes a marked acceleration in failure times compared to distilled water [23, 24]. Brown was able to show that the solubility parameter of polyethylene (16.4 $MPa^{1/2}$) was quite close to that of the detergent Igepal CO630 (20 $MPa^{1/2}$) demonstrating its aggressive nature [25]. When exposed to a stress cracking agent, the amorphous regions of a polyolefin are thought to plasticize and swell, concentrating internal stresses and encouraging further void formation. Ward et al. [26] performed their own ageing studies, comparing the facture times of an ethylene-octene copolymer in air versus Igepal at various temperatures. They found that in order for Igepal to actively affect the system, the time to failure must be beyond a critical time termed the Igepal Transition Time (ITT). Beyond the ITT, activation energy for craze formation was found to be reduced. This observation seems consistent with the *multiple* crazes observed by Lustiger and Corneliussen (Figure 4) after their polyethylene samples were exposed to Igepal for 30 hours. Ward et al. also proposed a more technical explanation behind ESC by linking the activation energy for SGC in polyethylene (100 kJ/mol) to the α-transition noted by Boyd, suggesting ESC is also crystal dependent [26, 27]. They believe the ITT is related to the diffusion of Igepal into the crystal lamella, and propose that this process enhances ESC where Igepal acts as a *lubricant* by increasing the mobility of TMs, increasing the rate of disentanglement [26]. Beyond the work described, more recent research has been aimed towards finding polymeric properties that could be tuned to improve overall ESCR.

Huang and Brown were able to show that polyethylenes with a larger molecular weight fractured at a higher critical stress under a fast fracture technique (Figure 6) [28]. This observation was related back to tie molecules, where it is postulated that a critical molecular weight must be met for tie molecules to form. The authors then proposed a critical M_w = 18,000, as they were not able to observe any TMs below this value [28]. Soares et al. were later able to confirm Huang and Brown's findings by directly comparing the ESCR of multiple molecular weight polyethylene samples by performing the Bent Strip Test (ASTM D1693) [11] .

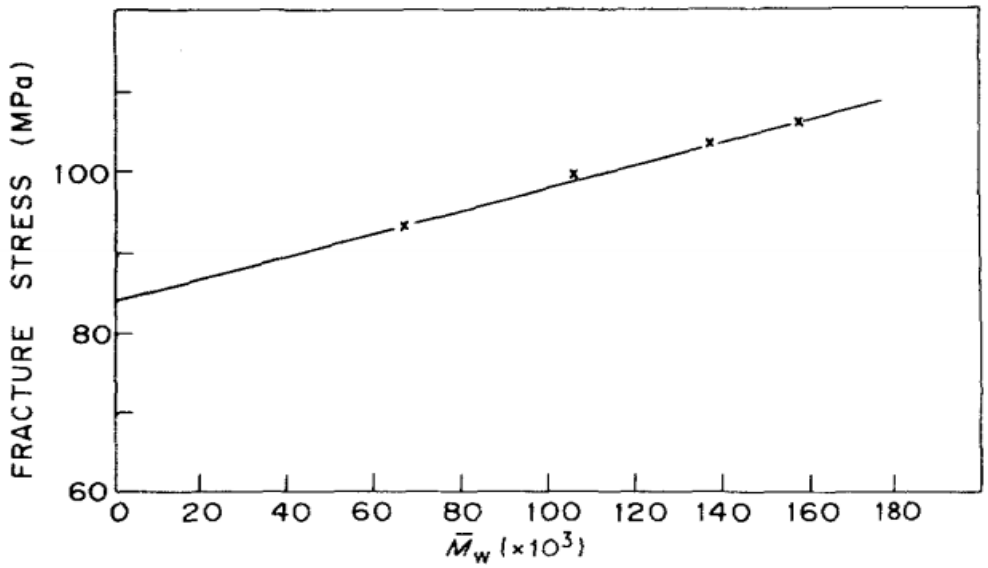

Figure 6: Larger molecular weight polyethylenes have a larger fracture stress when tested under a fast fracture technique using liquid nitrogen. Adapted from [28]

Besides the molecular weight of polymer chains, chain branching is also a valuable property for determining the ESCR of polyolefins. Huang and Brown were able to show that by increasing the n-butyl branches on an ethylene-hexene copolymer from 0 to 4.6 butyls/1000 carbons, the rate of SCG decreased by a factor of 10^4 [29]. It is thought that chain branches are able to decrease the average lamellar thickness, meaning the critical M_w to form TMs would also decrease, increasing overall TM formation probability. Yeh et al. [30] added to this by comparing the effects the length of short chain branches had on ESCR. The authors were able to show that the presence of short chain branches increased the ITT,

indicating slowed diffusion of Igepal into the crystalline region. More interestingly, they found that between samples of similar crystallinity, branch frequency, molecular weight, TM density, but different short chain branch length, ITT did not vary. The final ESCR value did however increase significantly with longer branch lengths, owing to increased sliding resistance in the interlamellar amorphous region by an increase in chain entanglements [30].

Since the amorphous region has been determined to be the main area associated with semi-crystalline polymer strength and crack resistance, not much work has been done concerning crystal structure and ESCR. One must consider factors from both domains when investigating ESCR as tie molecules, and entanglements in general, arise from the lateral surfaces of lamella. Cheng et al. [31] realized properties of the crystals should be accounted for and successfully related lateral lamellar surface area to ESCR. Figure 7 is presented from their research, where it can be seen larger lamellar area contributes to higher ESCR as the probability to form TMs and entanglements increases.

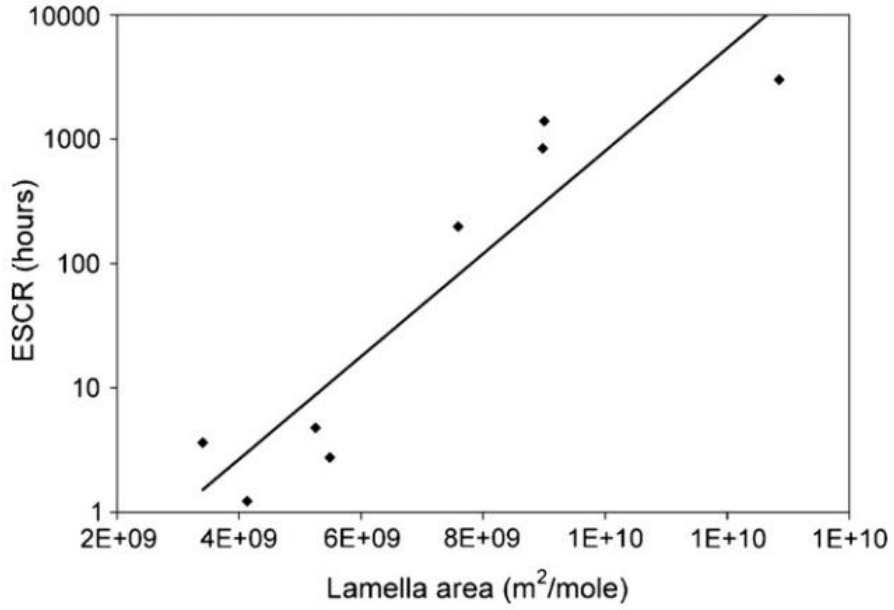

Figure 7: Environment stress cracking resistance improves with lager lamellar surface area. Adapted from [31]

Experimental Methods

Selected Materials

Polymers

Seven grades of polyethylene were used throughout the study, all coming from the same supplier of Imperial Oil Ltd (Sarnia, Ont.). All materials used were received as pre-molded square plaques of 17.5 cm x 17.5 cm x 0.3 cm dimensions produced according to procedure C of Annex A1 in ASTM D4703. Individual rectangular samples of varying dimensions were milled from the plaques for testing purposes. A summary of material properties of all polyethylene grades can be seen below in Table 1, with data quoted coming from the supplier.

***Table 1**: Summary of key material properties for all resins used in experimental work.*

GRADE	TYPE	DENSITY (KG/M^3)	MFI (G/10 MIN)	ESCR (F_{50} HOURS)[2]
1	Homopolymer (HD)	965	8.2	3
2	Hexene Copolymer (HD)	950	33	0
3	*Not Determined*	955	0.4	104
4	Bimodal Copolymer (HD)	956	0.3	370[3]
5	Hexene Copolymer (HD)	941	2	40
6	Hexene Copolymer (LL)	938	3.3	60
7	Hexene Copolymer (HD)	948	5	20

Ageing Fluids

The main ageing fluid used was Igepal CA630[4] (Nonylphenoxy poly(ethyleneoxy) ethanol) obtained from Sigma Aldrich CAS # 68412-54-4 or Igepal CA630 from Alfa Aesar CAS # 9036-19-5. Biodiesel was pure tallow-based methyl ester prepared from animal renderings supplied by Rothsay Biodiesel Inc.

[2] Values were determined from ASTM D1693
[3] Condition C of ASTM D1693 was used (100% Igepal at 100°C)
[4] Igepal CA630 can be used as a substitute for CO630 [32].

Ultrasonic Testing

Hardware

The heart of all ultrasonic based testing was a custom built computer, running a Xeon 5130 2.0 GHz CPU and 8.0 gigabytes of ram. A 1 terabyte size hard drive was required as continuous sampling of data was proven to quickly take up large volumes of storage space. To facilitate data acquisition, a 12-bit 4-channel simultaneously poling DAQ card (National Instruments®), capable of sampling at rates up to 10 MHz was used. For passive acoustic testing, the detection of events was performed with either a broadband F30α or resonant R30α transducer sourced from the Physical Acoustics Corporation. Detected signals were amplified through a Physical Acoustics 2/4/6c amplifier with optional amplification settings of 20, 40, or 60 dB. When performing active ultrasonic testing, an Olympus® 5077PR pulse generator was used which was capable of producing a tunable negative square wave with available pulse voltages of 100-400 V and pulse frequencies of 500 kHz-10 MHz to allow optimal signal transmission through a desired sample. A Panametrics NDT C604 (2.25 MHz – 1.0”) transducer was used for efficient generation and detection of active MHz signals through polymer samples when coupled with the 5077PR.

Software

Control of the DAQ unit for passive acoustics testing was accomplished through a custom software package written in LabVIEW. The LabVIEW program allowed for programmable sampling rates and a tunable signal threshold for determining if a detected signal should be written to file. As the software is capable of data acquisition at MHz rates, to mitigate heavily taxing the computer through continuously writing the acquired data to a file, the signal threshold acted as a filter to prevent the storing of constant background noise. However, when the filtering threshold was exceeded, the program took a fixed sized packet of data and wrote it to a TDMS file in a user-determined directory. Every event detected was written to its own file with a title that contained the absolute time the event had occurred. Analysis of

recorded acoustic events was done using custom Python code built upon multiple libraries capable of processing TDMS file formats and performing signal processing operations.

Quantification of active ultrasonic testing parameters was also performed through a custom built program with LabVIEW software. A test was conducted at the click of the mouse, where the LabVIEW program was used to initiate an excitation voltage from the DAQ board to trigger the 5077PR for emission of the main ultrasonic signal for determination of both ultrasonic velocity and attenuation values. Concurrently with the excitation voltage, the program was set to initiate data acquisition at a user defined sampling rate (10.0 MHz) for a specific period of time (0.1 s) to record the main acoustic pulse and the resulting echo. A user defined threshold was also used for signal analysis to signal the start of each signal for computation of velocity and attenuation values. The user was responsible for measuring and inputting the thickness of each sample to ensure accurate velocity values as calculated through Equation 1.

$$Eq\ 1: \qquad Ultrasonic\ Velocity = Sampling\ Rate \cdot \left[\frac{2 \cdot Sample\ Thickness}{\Delta t}\right]$$

Materials Testing

Differential Scanning Calorimetry

A Q200 differential scanning calorimeter (TA Instruments) was used for identifying the thermal transitions and crystallinity of each polymer resin. Testing for all samples utilized a temperature range of 40 – 200°C with a heating ramp rate of 10°C per minute. Polymer samples were ensured to weigh between 5 – 7 mg and the theoretical heat of fusion of 100 % crystalline polyethylene used was 290 J/g [33].

Tensile Testing

Mechanical properties of the polymer resins were evaluated with a Model 3366 Universal Mechanical Testing Machine from INSTRON Corporation. Primarily tensile testing was performed on the

rectangular samples to obtain stress-strain data for computation of Young's Modulus and determination of the yield point. A standard cross-head speed of 5.00 mm/min was used for all tests.

Microscopy

A Keyence VHX-5000 digital microscope was used for imaging polymer samples during environmental stress cracking testing. Good quality 1600x1200 digital pictures of polymer fracture surfaces could be obtained with the 20x-200x lens utilizing various image-stich algorithms. The tiling head of the microscope allowed images to be taken of bent samples.

Environmental Stress Cracking Resistance Testing

Primary determination of ESCR values was the traditional Bell Test (ASTM D1693), where replicating these testing conditions provided an in-house verification method and benchmark by which other tests could be compared. The specific instruments needed for sample fabrication and preparation (die, notching jig, bending apparatus, brass retaining channels) were sourced from Custom Scientific Instruments Inc. Condition A guidelines were followed (10% Igepal at 50°C and t = 3.00 – 3.30 mm) unless stated otherwise.

Development of a Passive Acoustics Testing Method for the Evaluation of ESCR

Introduction

One of the limitations of the Bell Test for evaluation of ESCR is the quantification of failure via a visual inspection. Considering the smallest object a human eye can resolve is roughly 0.03 – 0.06 mm in size, detection of a crack is limited to these dimensions. Of course, observation of early cracking on a white polymer surface makes visual inspection a rather unreliable metric, which brings about the need for an alternative. As stated previously in the Literature Review, the initiation and propagation of a polymer cracking event is accompanied by the release of energy intrinsic to the breakage of intramolecular linkages (tie molecules) and unraveling of entangled cilia. This burst of energy is marked by the propagation of a crack front, but also the formation of elastic waves, which would travel outwardly from the initiation point along the surface and internally of the material until being attenuated [34]. The key point being the detection and monitoring of elastic, or acoustic waves could be an alternative to the simple visualisation of crack propagation. This chapter discusses the implementation of a passive acoustics detection method for quantification of the ESCR of polyethylenes.

Testing Configurations & Results

Large Scale Tank

In conjunction with the software outlined in the Experimental Chapter, various testing configurations were used to isolate passive acoustic signals with the primary set-up designed to replicate the ageing conditions outlined in the Bell Test. The initial configuration took the form of a polymethyl methacrylate cylindrical tank of 17 & 3/8” diameter and 21” depth, which was connected to an external VWR Model 11575 water bath. As seen in Figure 8, the water level was kept between 8.25” – 8.5” to ensure complete coverage of the polyethylene test samples through a gravity drain system.

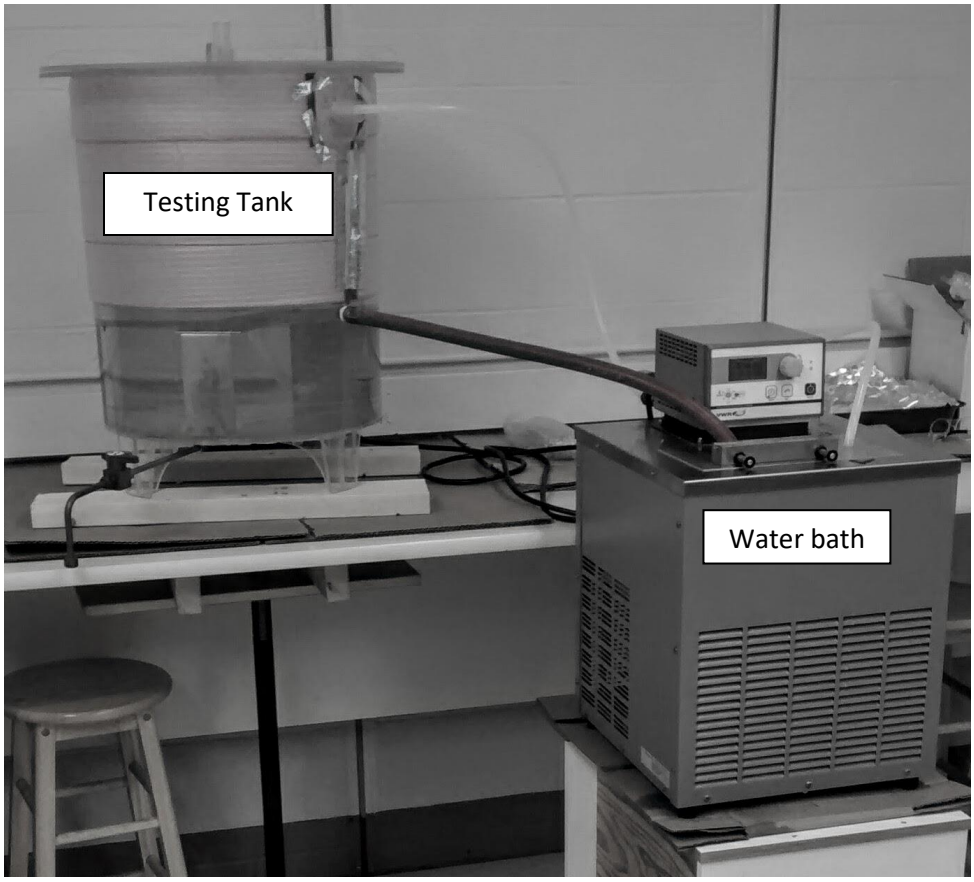

***Figure 8**: Initial Bell Test tank set-up with external VWR water bath highlighted.*

Reflectix™ type insulation wrap was secured around the water filled portion of the tank with Velcro® strips to stabilize temperature and provide quick access for sample viewing. A test tube rack constructed from galvanized sheet metal was used to hold the tubes containing samples in place. Overall, the testing system was capable of simultaneously evaluating nine independent resins, but only one at a time could be accommodated for acoustic monitoring. For efficient detection of acoustic activity the device in Figure 9 was manufactured where a brass cap was soldered to the standard u-shaped brass channel described in ASTM D1693. The brass cap functions as a low impedance mounting point for the acoustic sensor to facilitate good signal detection.

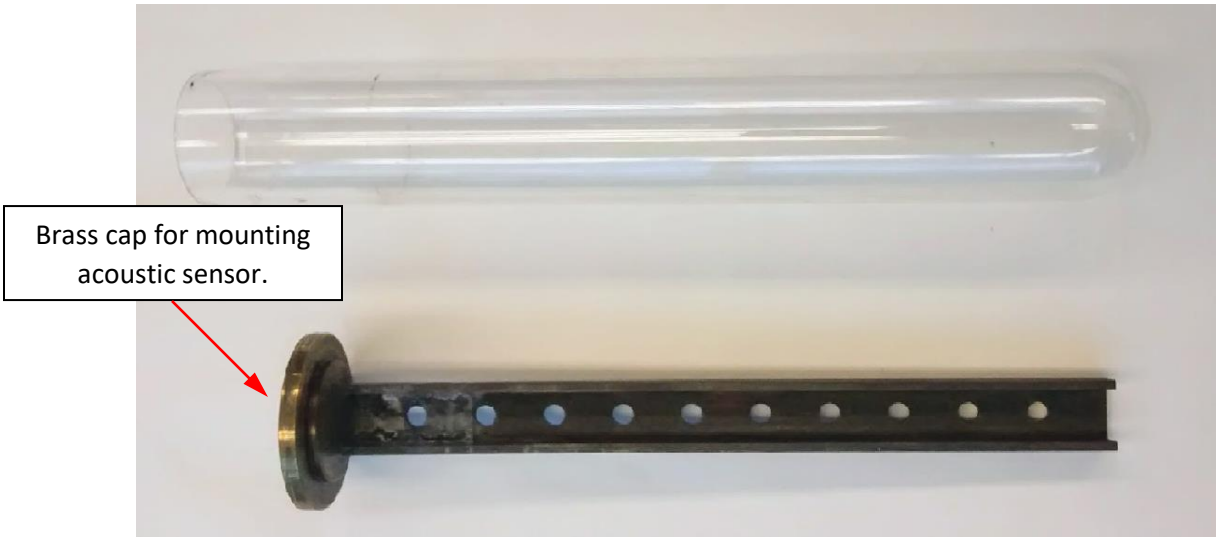

***Figure 9**: Sensor mounting device.*

During all testing cycles the acoustic sensor was covered with a sheet of Saran™ wrap to protect the electrical connections from the humid tank environment. A thin layer of coupling grease (Super Lube) was placed between the sensor and the brass cap for elimination of any air gaps for improved signal detection.

With the testing system finalized, ten samples of Grade 3 resin were punched out of a 17.5 cm by 17.5 cm plaque with an arbor press-mounted die and a small defect was created on each sample with a razor blade according to the ASTM D1693 procedure. The samples were bent and secured in the u-shaped brass channel (Figure 9) and immersed in a test tube containing a solution of 10% Igepal in distilled water. The acoustic sensor (F-30α) was then fitted onto the brass cap and the whole assembly was placed into the 50°C water bath. With everything in place, the DAQ was set at a 2.0 MHz acquisition rate, and a detection threshold of 0.06 V was used to filter signal from noise of the incoming 60 dB pre-amplified data stream; the voltage threshold was confirmed valid through countless trials of purposely cracking polyethylene samples in a tensile testing machine.

After 89 hours, all ten samples were visibly fractured, signaling the completion of the test. A total of 1390 acoustic signals were recorded with activity present over the entire testing period. Typical

acoustic signatures obtained can be seen in Figure 10, with some displaying prominent frequency domains below 20 kHz, while others show concentrated activity between 150 and 400 kHz when looking at the respective signal in the frequency domain by Fast Fourier Transform (FFT).

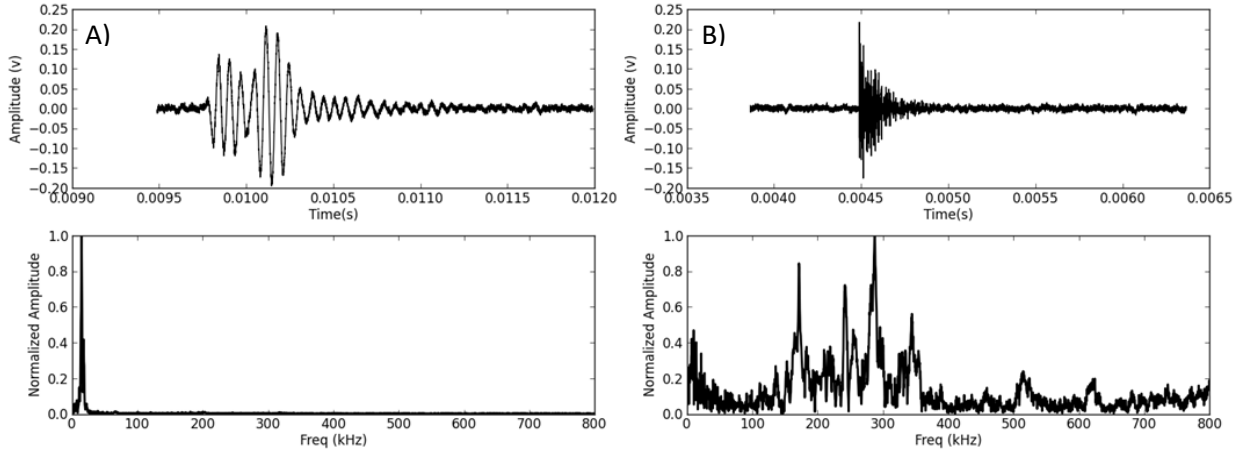

Figure 10: *Main acoustic signals obtained from the hybrid ASTM D1693 test. Low frequency dominant waveform is shown in (a), while high frequency dominant in (b). The top portion of each plot is the actual recorded signal; the bottom is the respective FFT.*

Analysis of the normalized signals in Prosensus ProMV software with a principle component model utilizing two components showed grouping of low frequency signals (Figure 10-a), but no discrimination could be made between higher frequency dominant signals (Figure 10-b). From the model generated in ProMV it became apparent the system under investigation was rather complex and confirming the source of each signal would be a difficult task. More tests completed with this specific system were able to show signals deriving from the disturbance of water draining from the tank into the circulating water bath, Velcro® related cracks/snaps, drops of condensed water falling from the tank lid, thermal effects and electromagnetic interference (EMI). The contribution of unwanted acoustic activity indicated a simpler system needed to be created.

Single Heated Sample Testing – Mason Jar

To try and eliminate some of the interference problems related with the large PMMA cylindrical tank, a water filled Mason jar on a hot plate was utilized to allow evaluation of one test tube only (Figure 11). An experiment involving two samples of Grade 7 monitored with the F-30α sensor at a

sampling rate of 2.0 MHz produced 107 events after 18 hours of testing. Similar to the large tank set-up, positively identifying an event related to stress cracking was unfortunately not possible. All the 107 events recorded were visually indistinguishable; a sample signature can be seen in Figure 12 with most following the appearance of low frequency interference.

***Figure 11**: Simplified Mason jar testing configuration.*

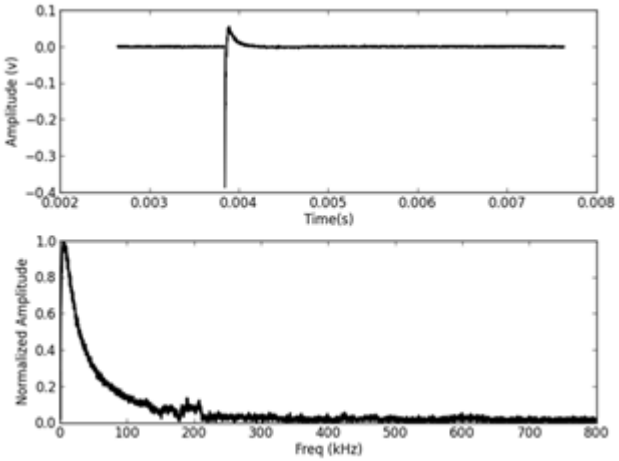

***Figure 12**: Typical noise signal obtained from the simplified set-up. Actual signal is represented in the top plot, with the FFT shown below.*

Subsequent tests with no polymer samples produced a total event count similar to tests with polymer, indicating noise was still actively being recorded. Some sources of noise was found to be the electromagnetic interference (EMI) associated with the hot plate turning on/off during temperature regulation and possible inconsistent voltage supply running the DAQ system. Discussions with the sensory supplier could identify no equipment causes that would eliminate these artifacts. Once again, it was decided to further simply the test system for elimination of noise sources.

Alternative Transducer Coupling Configurations

A more direct method of mounting the sensor (Figure 13) was designed for better acoustic detection over the brass cap method seen in Figure 9.

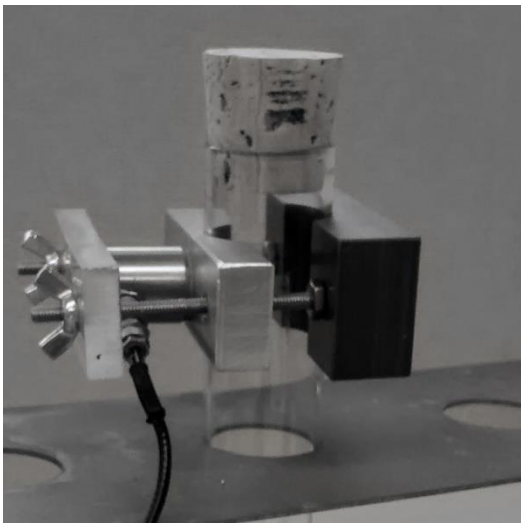

***Figure 13**: Alternative acoustic sensor mount for more direct detection of fracture evens during stress cracking tests.*

The sensor shown in Figure 13 was clamped onto a piece of aluminum machined to match the contours of the test tube. Coupling grease (Super Lube) was used between all mating surfaces to eliminate air gaps for efficient acoustic energy transfer. The test used one sample of Grade 7 resin, with the F-30α sensor positioned in-plane to the sample in the brass u-channel. No heating was used during this experiment and isolation of the test tube from any stray vibrations was ensured by allowing the tube to rest on a thick piece of fabric. An uninterruptable power supply (UPS) was also used to offer some conditioning of the incoming power. The test was run overnight for approximately 16 hours, with 91 events recorded. Unfortunately, the system was unable to capture any sample related activity, with all events having a signature similar to Figure 10-a, indicating EMI noise despite implementing the UPS. Due to the volume of noise related events recoded, the practicality of adopting this hybrid approach may not be a viable alternative as the nature of ASTM D1693 requires long testing times, which based on the set-up used, would amount to a tremendous amount of data for analysis. It is thought that since ESC is a type of brittle fracture, which follows a slow crack growth mechanism, the energy released during craze initiation/propagation may be so small it attenuates or scatters before it reaches the acoustic sensor, making it impractical to detect with the current set-up.

Small Scale Tank with Video Monitoring

To further confirm the possibility that accurate detection of passive acoustic events was beyond the capabilities of the system hardware, another testing configuration was designed around a rectangular tank of 40 cm length by 25 cm wide by 30 cm deep for adaption of the Bell Test. In place of the VWR water bath was a Lauda MT Immersion Heater Circulator, which was mounted directly to the tank wall for quick and efficient heating. The tank was covered on three faces with black Bristol Board to improve picture resolution, as video monitoring was used in conjunction with the passive acoustics. A depiction of the improved set-up can be seen below in Figure 14.

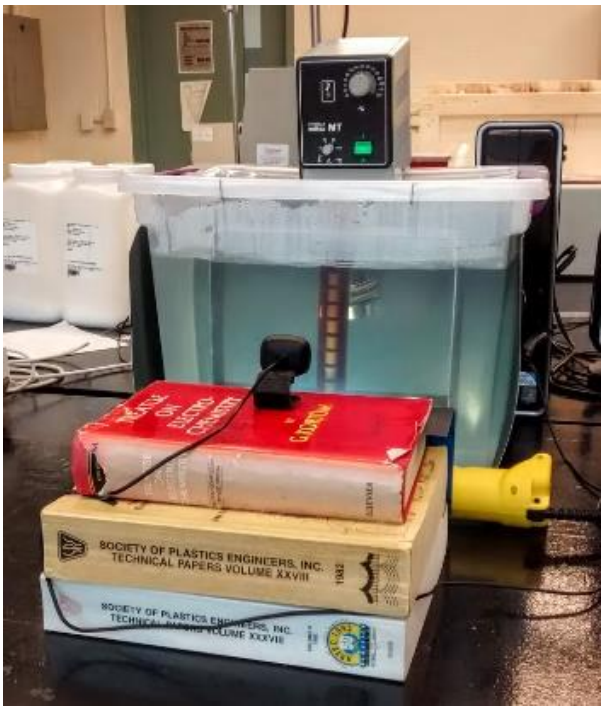

Figure 14*: Second generation Bell Test set-up constructed from rectangular plastic tank. Immersion heated, web-camera and addition lighting was used to improve failure detection.*

With the newly designed system, a test was performed using two R-30α sensors: one was clamped to a brass u-channel containing six samples of Grade 1 resin, while the second sensor was clamped to another brass channel containing *no polymer samples* to act as a control. A depiction of the testing apparatus housed within the rectangular tank can be seen below in Figure 15.

***Figure 15**: ESCR Test used to identify possible sample derived acoustic activity.*

Despite the previous findings of there being a constant threat of interference signals masking the passive events derived from the polymer, it was hypothesized for this test that since both sensors were subjected to the same environmental conditions, interference should be detected by both sensors at the same time, making it theoretically possible to isolate passive events associated with the polymer. A new LabVIEW virtual instrument was created to record the acoustic events detected from each sensor to their own separate file. The system was run at an acquisition rate of 2.0 MHz under 40 dB amplification, while the threshold for recording/saving event data was still 0.06 V for both sensors as used in previous tests.

A depiction of the samples at the start and after 4 hours of ageing can be seen in Figure 16, with the circled area highlighting the rather extreme cracking that can occur for Grade 1, which is known for having a poor ESCR value of only 3 hours.

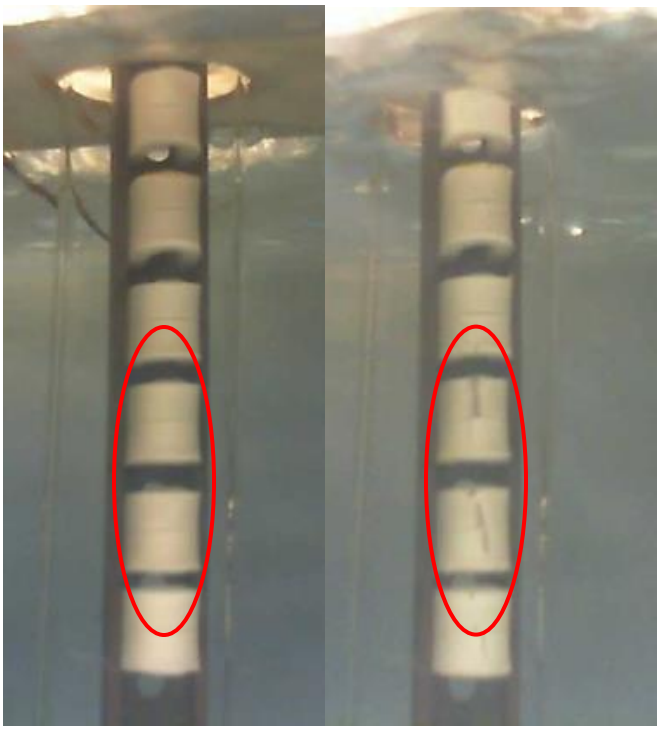

***Figure 16**: Comparison of Grade 1 pre and post ageing in a 10% solution of Igepal and water. Extensive cracking after a short period of time (4 hours) is highlighted.*

After the test was completed it was found that the sensor monitoring the polymer had recorded 6 events, while the sample independent sensor unusually recorded 27. This nearly five times difference in favour of the test tube containing no samples was the complete opposite of what was expected and further confirmed the inability to detect and identify a polymer derived acoustic event. Some explanations for this outcome could be a difference in sensitivities between the sensors, or simply the placement of each test tube within the tank; the control test tube could have been subjected to a more intense flow field which contribute to more acoustic activity.

Conclusions

All the testing methods investigated were successfully able to produce cracking events in multiple grades of high density polyethylene. Passive acoustic events were recorded, however after analyzing the signals it became apparent that multiple signal sources for the events existed for different

testing environments. Continued simplification and refinements to remove noise sources were fruitless, making positive identification of a polymer based acoustic event highly unlikely.

To reiterate, it is believed that the slow crack growth mechanism across all resins is a progression of small micro events marked by tie molecule breakage and interlamellar cilia unraveling. The events of slow crack growth progression release small bursts of energy, and the elastic waves associated with these events are quickly attenuated, making detection by a sensor mounted a distance from the point of initiation difficult. The findings from the passive testing systems indicate that if this method of detection were to be pursued, the set-up may need to be altered to accommodate the placement of a sensor directly on the polymer sample, as this would allow the best chance of polymer derived signal detection. However, this could be rather difficult due to the confinements of the testing system and the harsh environment the sensor could be subjected to, making this approach rather impractical. An alternate approach with active acoustics is discussed in the next section which utilizes direct placement of an ultrasonic transducer on a polymer surface and generation of a high amplitude reproducible elastic wave.

Development of an Active Acoustics Testing Method for the Evaluation of ESCR

Introduction

Having concluded in the Passive Acoustics Chapter that detection of polymer derived acoustic signals was impractical due the material's attenuating nature and the low energy released during a cracking event, it was decided a different approach was needed to probe for failure detection. Active acoustics, or ultrasonic probing is a growing field that relies on the generation and interpretation of ultrasonic waves in an object under investigation through one or multiple transducers. This diagnostic technique is used in countless areas with methods such as guided Lamb waves monitoring the onset and progression of fatigue cracks in airplane skins or detection of anomalies in boiler pipes and furnaces [35, 36]. Most systems have been adopted for use around low attenuating materials such as metals, as signals can travel large distances without compromising resolution. Some work has been done with polymers, as Piche has shown that the measurement of velocity in a sample of polyethylene is proportional to the material's density [37]. Working with the same principles as Piche, this section details an analysis technique whereby ultrasonic velocity and attenuation values of a polymer is attempted to be related to its environmental stress cracking resistance.

Testing Configurations and Results

To study the use of ultrasonic parameters for identification of ESCR properties, an experiment was conducted where samples of Grades 1, 2, 4 and 6 were aged in solutions of toluene, 10% Igepal in de-ionized water, and B100 biodiesel. Fluids other than Igepal were used to try and provoke a variety of material responses, which was hoped to be detectable though ultrasonic probing. Only one sample of each Grade was used per fluid type and all samples had a rectangular shape measuring ~20.0 mm wide x 180.0 mm long x 3.0 mm thick. Sample ageing was conducted over a period of 124 hr at room temperature while mass, ultrasonic velocity and attenuation measurements were taken pre-ageing and post-ageing after 1, 6, 24, and 124 hr; unlike the previous methods in this thesis, the sample was not

immersed in any fluid at the time of the acoustic analysis since now the sensors were in direct contact with the polymer. An ageing period of 124 hr was chosen as Gomes et al. were able to infer morphological damage in polyethylenes after only 72 hrs of ageing through frequency analysis of tensile generated passive events [38]. It was hypothesized that ultrasonic probing could improve on frequency analysis techniques by detecting signatures of age related structural damage (ESC) before performing a destructive tensile test.

The ultrasonic parameters were measured using the same DAQ system described previously, however it was now coupled to the Olympus 5077PR pulse generator. LabVIEW software was used that facilitated data collection under a pulse-echo mode, as this was thought to be easier compared to a pitch-and-catch method as only one transducer was needed. For optimal signal generation and acquisition, the pulse generator was operated at a frequency of 2.25 MHz (i.e. the transducer's peak frequency) with 20.0 dB signal amplification and the application of a high pass filter with a cut-off frequency of 1.0 MHz. Due to the thin sample thickness of only ~3.0 mm, the DAQ was run for only a short period of time (0.1 s) at an acquisition rate of 10.0 MHz as this was found to give good resolution.

Triplicate mass measurements were obtained with a Mettler AE200 4-point precision balance after thoroughly wiping clean any residual ageing fluid. A summary of the relative mass changes for the studied resins can be seen in Figure 17.

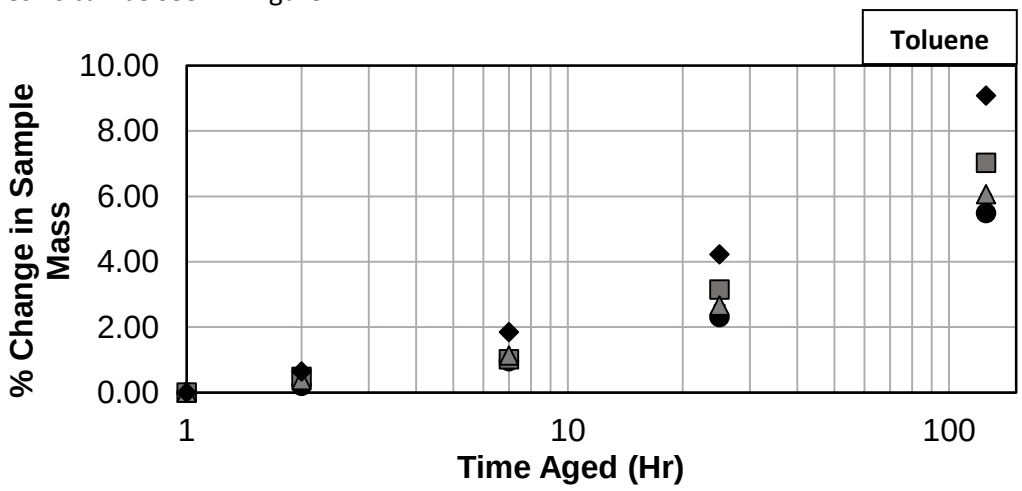

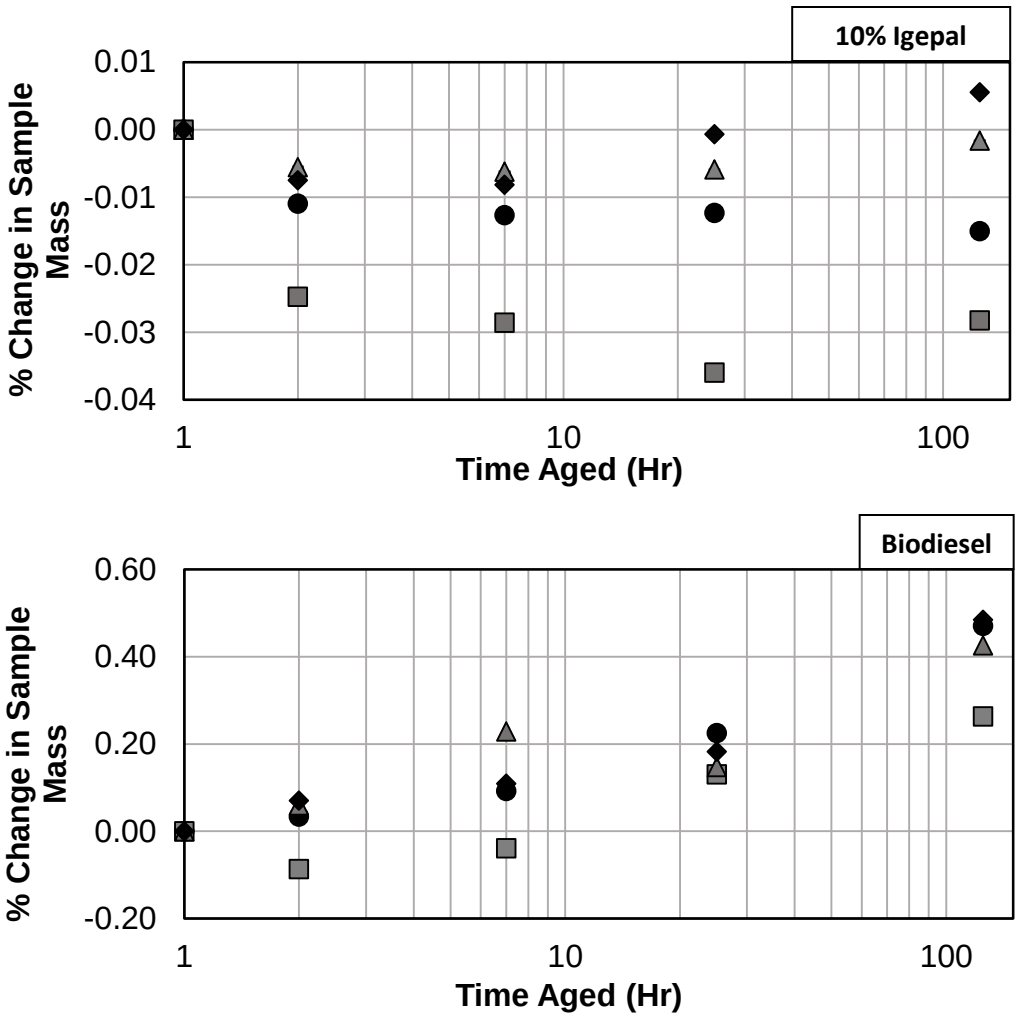

Figure 17: Comparison of relative mass changes for resin Grades 1, 2, 4, and 6 after ageing for 124 hr in solutions of Toluene (**Top**), 10% Igepal (**Middle**) and B100 biodiesel (**Bottom**). The relative standard error for the measurements was ± 0.02%. ● = Grade 1, ■ = Grade 2, ▲ = Grade 4, and ◆ = Grade 6.

The capacity for penetration of the fluids within each resin is quite apparent, with toluene accounting for the largest mass gain for all material studied. Of the four Grades investigated, Grade 6 being the least crystalline (57%) absorbed the most toluene, with a relative mass gain of approximately 9.0%. This observation follows the assumption that these fluids could only plasticize the amorphous region without penetration and dissolving the crystals, thus resulting in polymer swelling. Coincidently, Grade 1 being the most crystalline (82%) showed the smallest weight gain with a relative change of approximately 5.5%. Grade 7, and 4 fell between the two extremes of Grades 1 and 6, with relative mass gains of ~ 6.0% and 7.0% respectively with toluene.

Unusually, the 10% Igepal solution was seen to have no effect on the any of the polymer samples with mass changes in the range of only a few hundredths of a percent corresponding to the standard error of the measurement. This result was unexpected as the literature continually refers to Igepal as being a prime example of an aggressive stress cracking agent. The ageing tests were conducted in a static state (no force application), which indicated an active stress may be a critical factor for diffusion of Igepal into the polymer to induce stress cracking [24].

The B100 biodiesel was seen to provoke behaviour between that of toluene and Igepal, with changes becoming apparent after 6 hours of ageing. Similar to toluene, Grade 6 showed the largest change in relative mass with a 0.5% increase after 124 hours of ageing. Grade 1 and 4 were similar to that of Grade 6, while Grade 2 seemed to be the least influenced by biodiesel with only a 0.3% mass gain. Based on these results, it appears biodiesel is able to plasticize polyethylene, but not as effectively as toluene.

After each sample was aged, a simple ultrasonic test was conducted using the equipment described previously. The Olympus transducer was clamped to each sample using glycerol as the couplant. Glycerol was decided upon rather than the viscous vacuum grease (Super Lube), as over time the grease was seen to slowly thin out such that the ultrasonic velocity values were seen to increase, due to the lower impedance between the two surfaces (transducer face & polymer surface). Once the sample was clamped in place, five measurements were taken for both ultrasonic velocity and attenuation measurements (reported values were the average of the five samples). The total time for conducting the ultrasonic tests and mass measurements was kept to a maximum of 10 minutes to minimize error/diffusion of absorbed fluid out of each sample. A relative calibration curve (Figure A-1 of Appendix A) was also created using various known thicknesses of HDPE to provide accurate measurements of velocity directly though the LabVIEW code. A comparison of the results of the velocity tests can be seen below in Figure 18.

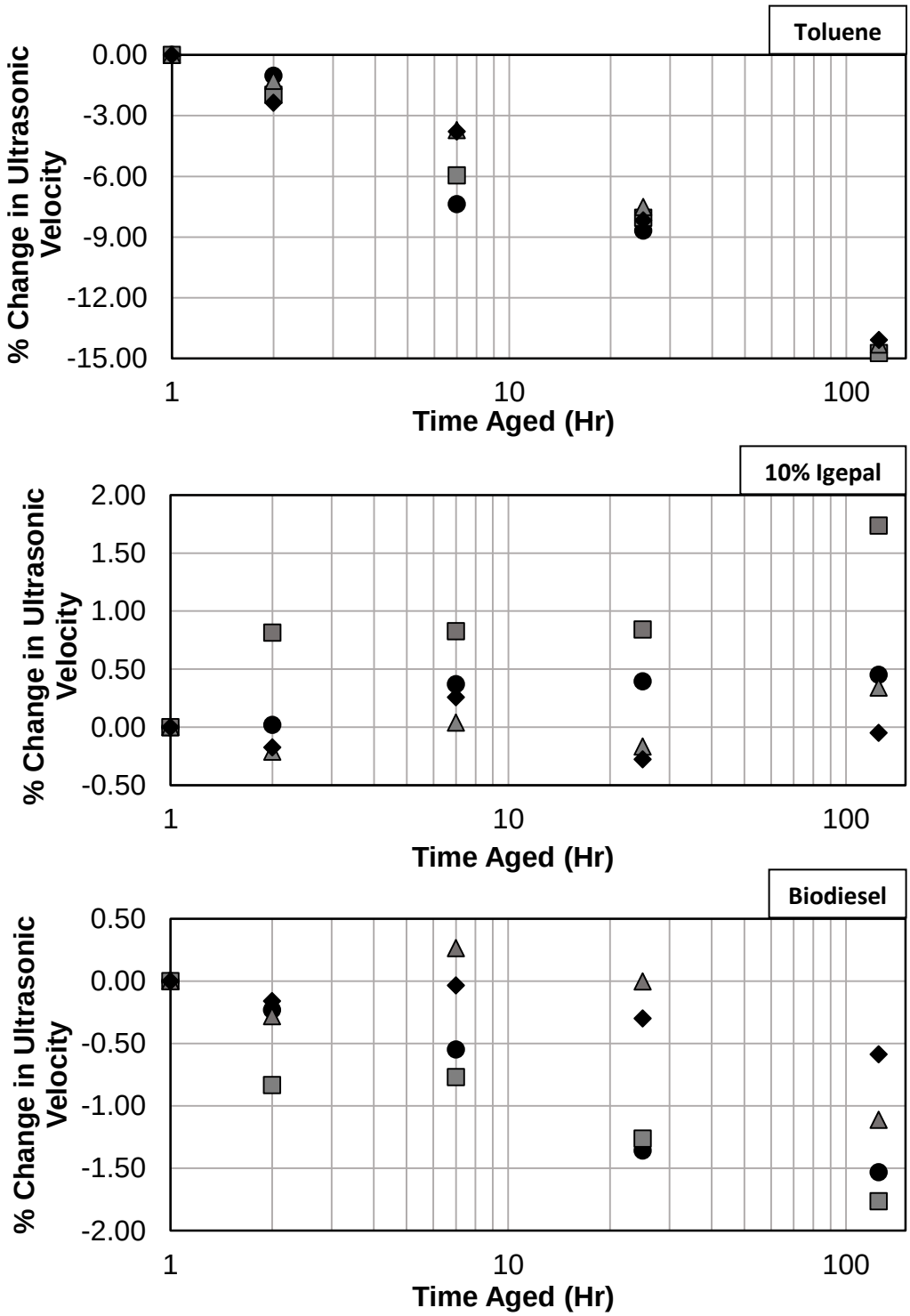

***Figure 18**:* Relative change in ultrasonic velocity for resin Grades 1, 2, 4, and 6 after exposure to either Toluene (**Top**), 10% Igepal (**Middle**) or B100 biodiesel (**Bottom**) after select periods of time. The relative standard error for the measurements was ± 0.02%. ● = Grade 1, ■ = Grade 2, ▲ = Grade 4, and ◆ = Grade 6.

The initial velocities of the virgin samples are as follows: G1 = 2578 m/s, G2 = 2401 m/s, G4 = 2465 m/s, and G6 = 2261 m/s (where G6 for example, corresponds to Grade 6). These velocity values agree in

magnitude with those found in literature for HDPE and also vary predictably with the density values of the virgin material [37]. The values seen in Figure 18 reflect the plasticization occurring to the HDPE samples after exposure to toluene, as a relative decrease in velocity of around 14.0% was seen for all material Grades. A relative decrease of 0.5 – 2.0% was also seen for the biodiesel aged samples, which again may relate to the early stages of plasticization. Interestingly, ultrasonic probing was found to be more sensitive at detecting aged related phenomenon compared to direct mass measurements as relative differences are nearly double for the aged materials. Based on these observations, it is believed that this technique can be used as a detection tool for plasticization.

No significant change in velocity was seen for any sample aged in 10% Igepal, and knowing that Igepal is a strong ESC fluid confirms this technique alone is not suitable for detecting age related structural damage, or evaluating a material's ESCR. A similar conclusion was found regarding attenuation values, no difference was found between the main bang and the first echo for all resins tested in the three fluids used. The comparison of attenuation values can be seen in Figure A-2 of Appendix A. Significant error between samples was also seen using the attenuation technique indicating poor reproducibility (virgin values for G2 ranged from 6.0 to 20.0 dB/cm), however values remained consistent with regards to the same sample across an ageing test. It is unknown why such large variations would exist for the same material, differences in clamping force or couplant thickness should only cause minor variation and no major outliers were seen across the velocity values.

As the main experiments on the HDPE samples were done under static conditions, a final tensile test on each 124 hr aged sample was completed under active ultrasonic monitoring to hopefully provoke ESC behaviour compared to the prior tests completed under static conditions. The tensile test was performed on the INSTRON 3366 Tensile Testing Machine at a crosshead speed of 5.0 mm/min. The test was stopped after 2.0% strain was reached on each sample, and a 13.0 minute relaxation period followed. Ultrasonic probing was done within the grips of the tensile testing machine pre-test, after 2.0% strain had

been reached and finally after the 13.0 minute relaxation period; the sample was never removed from the grips until all ultrasonic testing was completed. The goal of the tensile test with active ultrasonic monitoring was to see if putting strain on the interlamellar linkages (entangled cilia and TM's) could provoke a reaction seen with either velocity or attenuation measurements. A strain of 2% was used to minimize plastic deformation and prevent errors of velocity deriving from sample thickness changes during elongation. A visualization of the changes in ultrasonic velocity for each Grade of resin can be seen below in Figure 19. Numbers 1-3 on the x-axis of the plots represent the time the measurement was taken, with 1 being before the test started (sample sitting in jaws of tensile tester), 2 is after the 2% strain had been achieved, and 3 after the 13 minute relaxation.

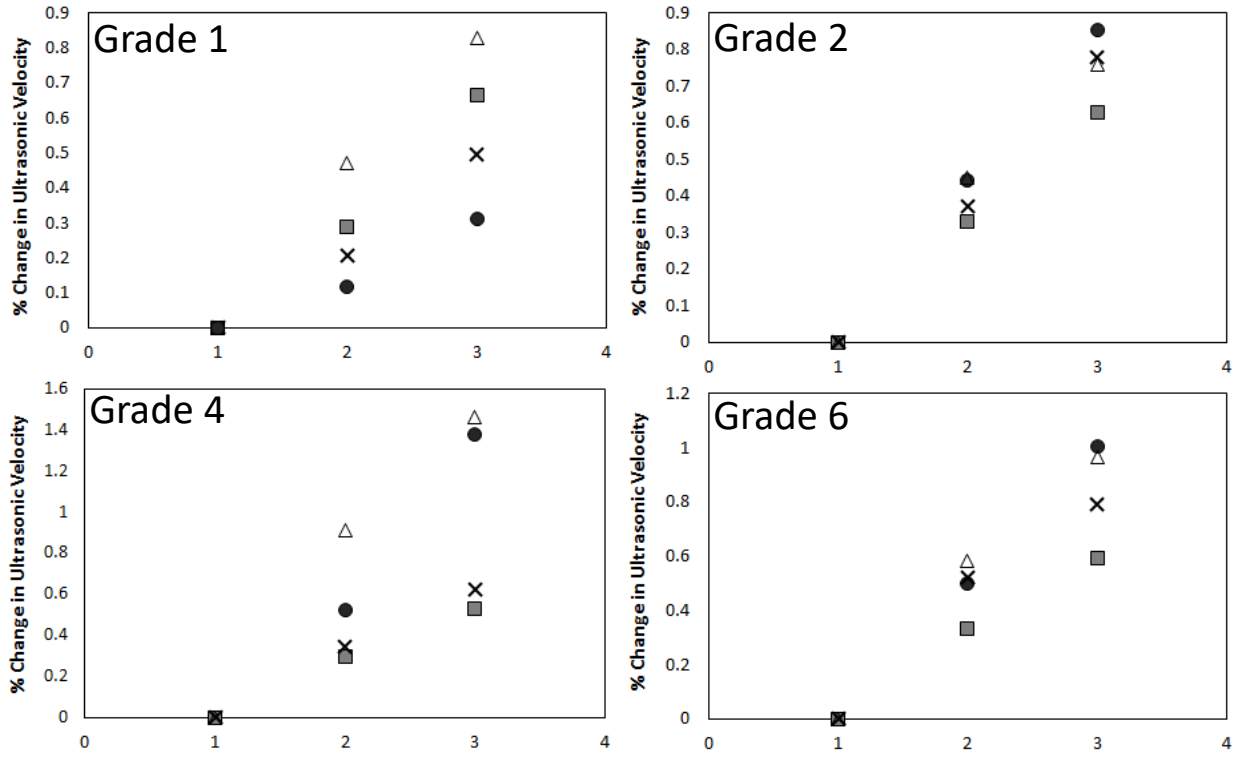

***Figure 19**:* A comparison of relative changes in ultrasonic velocity of HDPE resin samples during a tensile/relaxation test after ageing for 124 hours in specific environments. The symbols of the points corresponds to the environment, with ● = Virgin, ▲ = Toluene, ✕ = Igepal, and ■ = Biodiesel. Only one sample from each resin Grade was tested in the three environments. The relative standard error for the measurements was ± 0.01%.

The immediate observation seen in Figure 19 would be an increase in velocity both after the tensile and relaxation periods, which might be reflecting strain hardening behaviour of the material. Supplementary rheological tests were completed at varying Hencky Strains using an extensional rheometer (Xpansion Instruments) fitted to an ARES Rheometer to produce Figures A2 & A3 of Appendix A. Grade 6 showed strain hardening behaviour across all Hencky rates, while Grade 4 only seemed to produce strain hardening behaviour at higher rates (8 s^{-1}). Grades 1 and 2 did not show any strain hardening behaviour, which disagrees with the results of the active tensile test shown in Figure 19. The slight increase in ultrasonic velocity seen for all four resins may be reflecting geometric changes (sample thinning) rather than structural changes as was anticipated. The largest change in velocity of 1.5% for Grade 4 aged in toluene only reflects a magnitude difference of approximately 40.0 m/s (rather small). Considering the spread of changes in ultrasonic velocity seen with the active tensile test only spans a maximum of ~1.0%, this shows what was considered to be the inability of this technique for detecting morphological damage within a stressed polymer.

Even though ESC occurs over a much longer time scale than a ~15min tensile test, it was hoped ultrasonic probing could infer changes within the interlamellar region (stretched TM's, stressed entanglements), a key area relating to ESCR properties. Based on the observations from the active tensile test, it was concluded that *ultrasonic velocity is not a viable option for gauging environments stress cracking resistance of polymer resins*. The same result was found for attenuation values, with measurements remaining constant through the tensile/relaxation test.

An interesting supplement found though the tensile test is shown in Figure 20, with the effects of ageing on the elastic modulus of each material being represented. The plasticization caused by toluene is quite clear, with a large change in Young's Modulus for all materials, while both Igepal and biodiesel elicit small changes. Again, despite Igepal being a known strong stress cracking agent, standard mechanical

testing is not able to identify this nature, further indicating other testing situations needed to be investigated.

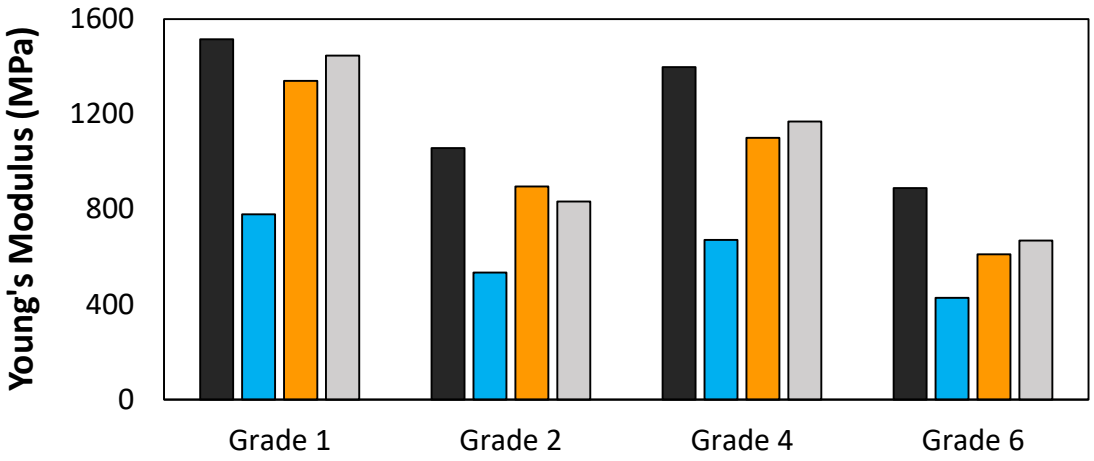

***Figure 20**: Elastic Modulus of each Grade of polymer resin after ageing for 124 hours in specific contacting fluids.*
■ = Virgin, ■ = Toluene, ■ = Igepal, and ■ = Biodiesel

Conclusions

Samples of Grade 1, 2, 4, and 6 resin were aged in fluids B100 biodiesel, toluene and a 10% solution of Igepal in de-ionized water for a period of 124 hours. Mass measurements and ultrasonic testing (material velocity and attenuation) were performed at predefined intervals to observe the effects each fluid had on the respective resins and to see if such a testing method could provide a reliable indication of ESCR. Results from both the mass and ultrasonic velocity measurements revealed the plasticizing (swelling) capabilities of toluene on the resins, with Grade 6 being the most susceptible and Grade 1 the least. The 10% solution of Igepal had no effect on the aged samples, while the B100 biodiesel began to show a measurable decrease in ultrasonic velocity (1-2%) after the final 124 hours of ageing. Attenuation readings were unusually sporadic and as such, were disregarded when interpreting results.

A tensile/relaxation test on the aged samples, with active ultrasonic velocity monitoring showed no measurable difference in ultrasonic velocity, with all samples changing by less than 1.5% (40.0 m/s). Based on the results, it was concluded that velocity measurements are not an appropriate tool for probing

changes in polymer structure such as the interlamellar region containing tie molecules and chain entanglements. No further work was conducted using ultrasonic probing systems for evaluation of environmental stress cracking

Development of a Force Based Measurement System for the Evaluation of ESCR

Introduction

It is known that the progression of microfailure events such as tie molecule breakage and disentanglement lead to the total failure of a polymer part. The investigation presented in the Passive Acoustics Chapter aimed to identity each individual micro event, however this was discovered to be complicated due to the noisy environment obscuring the low amplitude events. As most industrially accepted accelerated ageing tests operate by applying a load to a test piece (constant strain or force) and waiting for complete part failure, it was hypothesized that monitoring a polymer's response to an external force could reveal additional information for determining polymer ESCR. The following Chapter presents an alternative technique for monitoring micro events by looking as the response that a polymer has to an external force.

Active research is ongoing to develop force based systems for evaluation of ESCR, with a good example coming from a recent article by Jar and coworkers. Jar focused on developing a test around the absence of an inflicted stress concentrating defect as others have noted the variation in ESCR results that arise from this feature [39, 40]. The developed test, called the Plate Test, involved forced indentation of a 6.0 mm thick polyethylene sample with a 50 mm diameter indenter at 1.0 mm/min [40]; it appears to be an adaption of the blister test used in evaluating biaxial strain failure, mostly for metal stamping. Indentation was measured up to a fixed displacement of 41 mm and then the respective relaxation behaviour was monitored until visible cracking was apparent. An example of the force response curves can be seen below in Figure 21, where testing was completed in both dry (50°C air) and wet (50°C 10% Igepal) conditions.

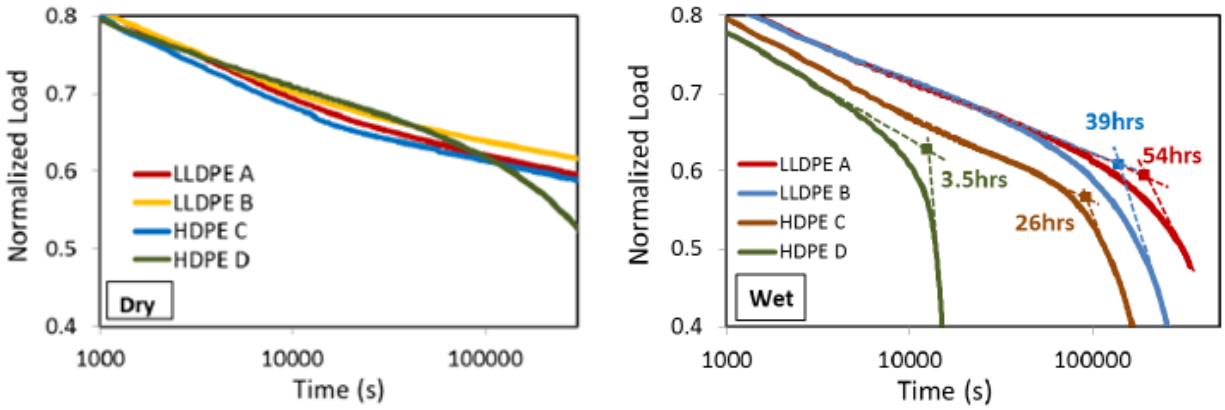

Figure 21: *Force response curves from the Plate Test ESCR evaluation technique. Figure adapted from [40]*

As seen in Figure 21, the change in load with time for the wet samples indicate the onset and progression of material failure much earlier compared to the dry environment. A rating for ESCR was quantified by extrapolating the linear portions of the force response curves to identify the knee point, where the on-set of ESC theoretically occurs. A comparison of Bell Test vs Plate Test ESCR rankings can be seen below in Figure 22, with significant time savings apparent.

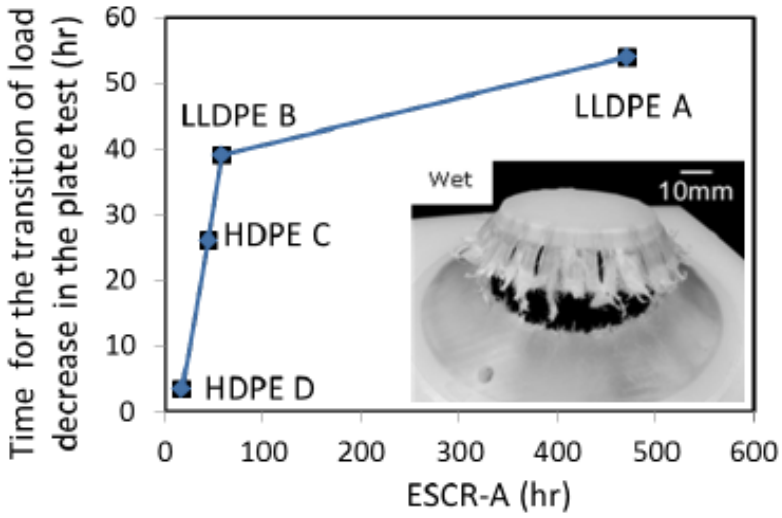

Figure 22*: Comparison of ESCR testing times for the Bell Tests and Plate Test. Figure adapted from [40].*

Despite how promising the Plate Test appears, questions arise involving test repeatability, maximum stress levels to ensure the absence of plastic deformation and the relevant of a biaxial tensile strain field. To rectify some of these issues, a second generation of the test was developed which used a

much smaller indenter of only 7 mm diameter and evaluated specimens of only 3 mm thickness [41]. The same indentation rate of 1 mm/min was used, however the displacement was scaled back to only 10 mm. Stress cracking is thought to occur in the samples due to the unique bi-axial loading imposed by the indenter and cracks form in the annular region in the direction of stretch (Figure 23).

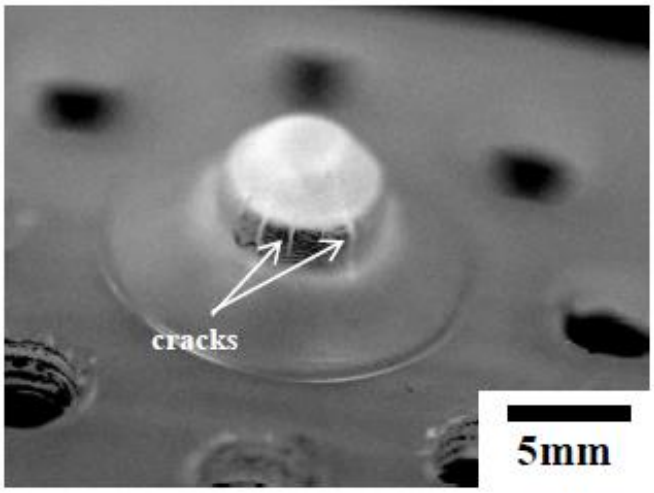

***Figure 23**: Visible stress cracks after an indentation test in a solution of 10% Igepal at 50°C. Figure Adapted from [41]*

Once again, a significant reduction in testing times were observed (even more so than the first generation plate test), however the main difficulty encountered was the method of failure detection. Observation of a failed specimen was quantified based on the bump, or change in rate of load decay once a sample was under relaxation. It was never directly stated, however it was assumed load monitoring was conducted with a mechanical testing machine and as such, **only one sample could be tested at a time,** which proves to be a disadvantage compared to the Bell Test.

Based on the information found through the development of an acoustic based monitoring test for evaluation of ESCR in polyethylenes and the work performed by Jar and coworkers on indentation testing, a novel force based measuring technique is described in the following section.

Preliminary Work

Understanding the simplicity and ease of obtaining ESC information using the Bell Test has made it industrially preferred despite its drawbacks, meaning an alternative technique would need to maintain these qualities while improving on known shortcomings, such as failure detection and test duration. Jar and coworkers had an excellent proposal to eliminate sample notching as Choi et al. showed the variations that exist when following the standard procedure of the Bell Test [39, 40]. Choi et al. however also showed notching consistency could be greatly improved by changing the mechanism from a fodder chopper type (Figure 1-A), to a guillotine style with removable shims to guarantee accurate notch depths [39]. The alterations proposed by Choi indicate the Bell Test could still be refined for improved ESCR ranking, therefore this configuration was used as the basis for specimen preparation in the testing technique proposed hereafter.

The imposed stress on a polymer sample undergoing the Bell Test arises from the material's opposition to being bent and retained in a strained configuration. The key observation being the opposing force provided by the polymer is *measurable*, thus it was hypothesized that this force could be used as a diagnostic parameter for determining ESCR. Much like the force curves generated by Jar, it was thought that an initial spike in load would be recorded after bending (straining) the sample, which would be followed by a rapid relaxation to an equilibrium plateau, and an eventual decrease in force due to crack initiation/propagation leading to sample failure.

To test the theory of force profiling, a KISTLER Type 9203 force sensor was configured to be used in a tensile mode for measuring the load produced by a strained sample. A 190 mm x 20 mm x 3 mm sample had 6.4 mm and 12.7 mm diameter holes punched through to allow placement of the sample around the sensor in a bent-strip configuration (Figure 24). During initial testing, sample notching and

bending was performed by hand which proved to be rather cumbersome as it was difficult to manually create a reproducible defect and afterwards secure the sample in position around the sensor.

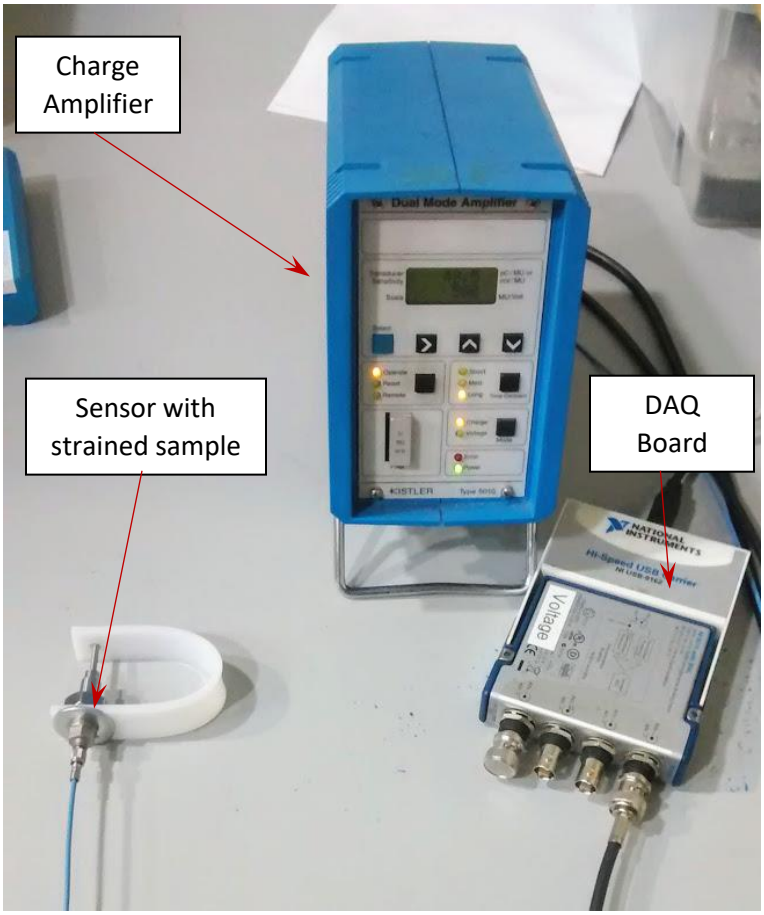

***Figure 24**: KISTLER force sensor with constrained polymer sample.*

The force sensor was connected to a KISTLER charge amplifier set to operate at a 10 N scale (high amplification), which was further connected to the data acquisition unit described in the Experimental Methods Chapter. A lower sampling rate (25 Hz) was chosen compared to the acoustics work as the entire failure process (slow crack growth) occurs on a longer time scale than individual acoustic events.

After bending and mounting of a sample to the sensor, the set-up was suspended over a glass container on a hot plate containing a 50°C solution of 10% Igepal in water. Trial runs were completed on Grade 1 resin over a period of 10,000 s (~2.8 hr) and the respective normalized force profiles can be seen below in Figure 25.

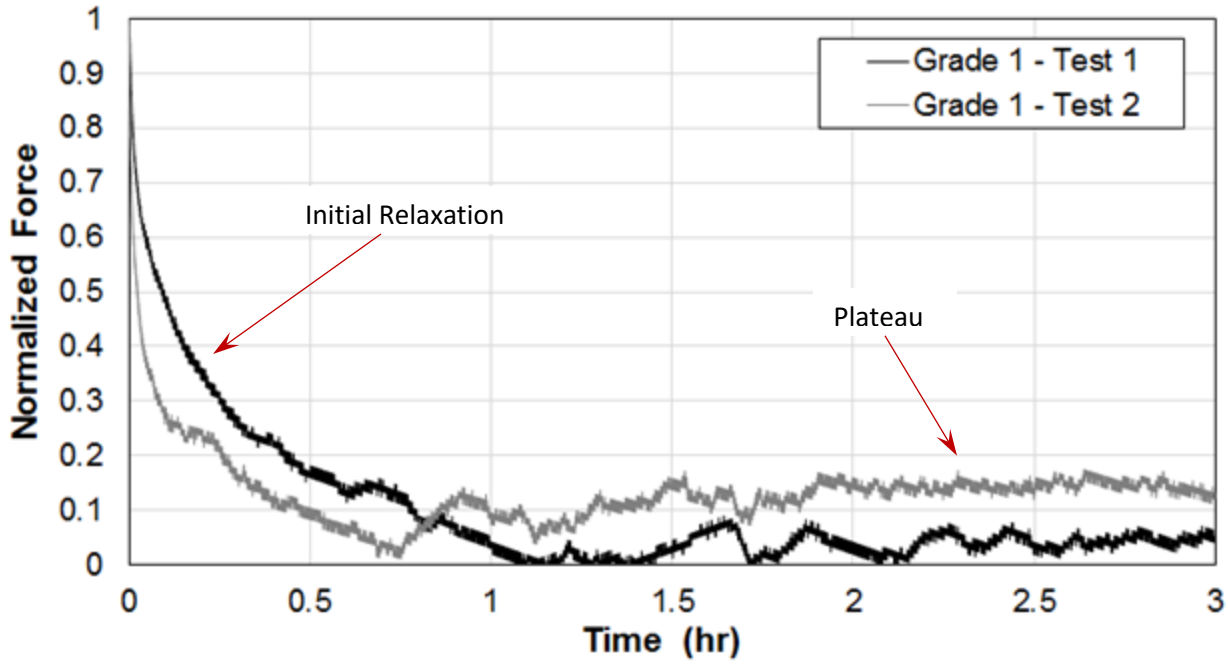

***Figure 25**: Force profiles obtained from KISTLER Sensor for Grade 1 resin aged in a 10% Igepal solution.*

The force profiles shown (Figure 25) revealed that loading strains are measurable over a lengthy period of time (relaxation and plateau regions highlighted), however the apparent noise and lack of a fracture signature was a concern initially. Measurement drift was also a noted problem with the KISTELR sensor as this required an extra processing step and also limited the testing time. Despite the noted problems with this sensor, the decision was made to continue investigation of this technique.

Effects of Sample Length on Failure Time

The excessive noise seen with the KISTLER sensor was a major problem, and to rectify the issue a voltage based OMEGA LCM703-10 10 kg load cell coupled to an OMEAGA CCT-80 load cell signal conditioner was used as a replacement. Both pieces of equipment can be seen pictured below in Figure 26 & 27, and were connected to the data acquisition system outlined previously. Samples were once again notched/bent by hand and restrained around the sensor to provide a measurable tensile force.

***Figure 26**: OMEGA sensor with mounted polymer sample.*

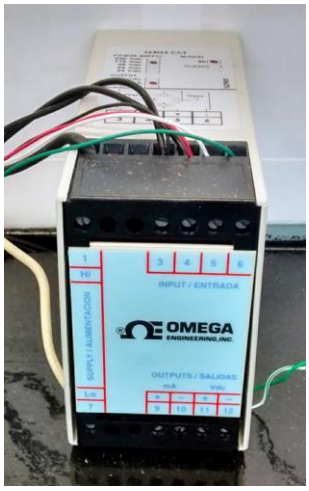

***Figure 27:** Load cell signal conditioner.*

To gauge the performance improvements provided by the OMEGA equipment, an experiment was conducted on Grade 2 resin, where samples of lengths 120, 130, 140, 150, 160, 170 mm (20 mm width, 3 mm thickness) were tested to observe which geometry provided the shortest failure time upon ageing in a 50°C bath of 10% Igepal. Logically, it was hypothesized that decreasing sample length would lead to a shorter failure time due to increased bending stresses (due to a smaller radius of curvature). A summary of the results can be seen below in Figure 28, where only 4 of the 6 samples are represented due to select samples not surviving the bending procedure.

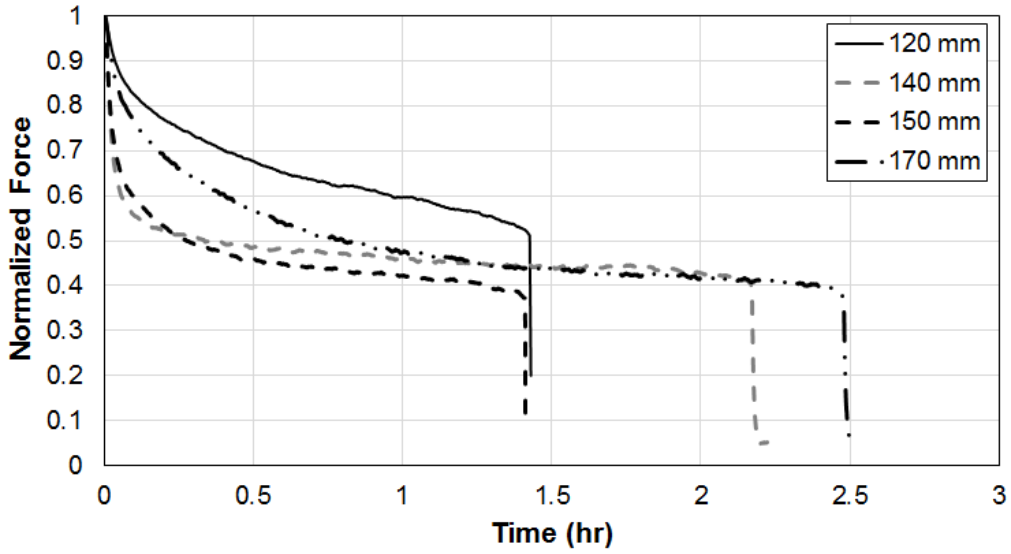

***Figure 28**: Failure profiles for varying lengths of Grade 2 resin after ageing in a 50°C bath of 10% Igepal solution.*

A difference in failure time by approximately 1.25 hr can be seen between the samples of 120 and 170 mm lengths, which agree with the hypothesis, however discrepancy can be seen with the 140 and 150 mm samples as the shorter sample (140 mm) took almost 45 min (0.75 hr) additional time to fail. The force profile of all the bendable samples show a very abrupt failure signature and the fracture site further confirmed brittle failure. This type of breakage was expected from Grade 2 resin, considering its high MFI (33) and designated ESCR value of 0 hours; however, repeats were considered necessary to clarify the atypical result witnessed between the 140 and 150 mm samples.

Six more samples were milled from a different compression molded plaque, and the same testing conditions were replicated as discussed previously. The resulting force profiles can be seen below in Figure 29, where all sample lengths were successfully tested.

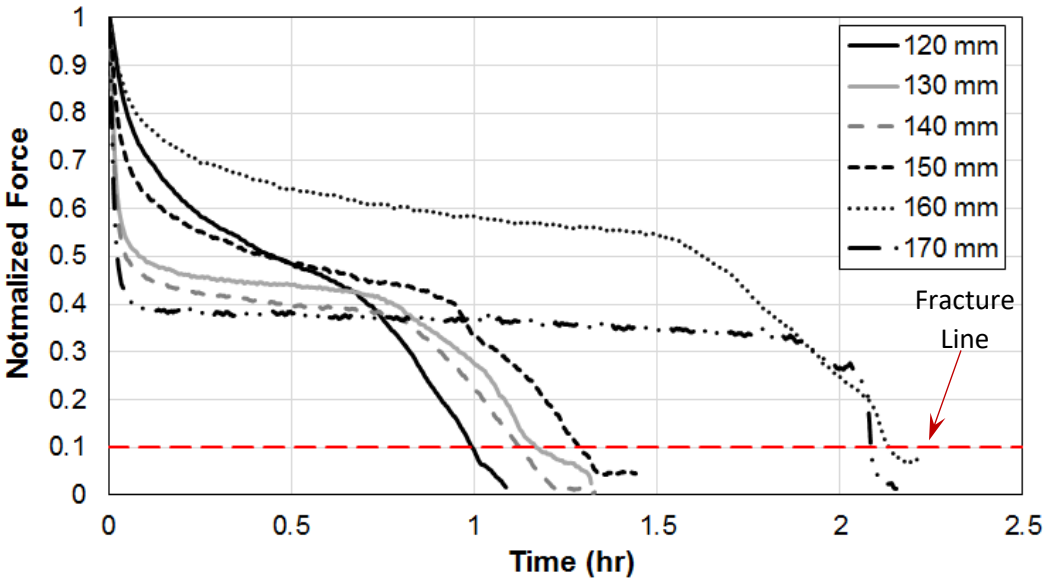

***Figure 29**: Re-run of varying sample length to determine optimal failure time. Fracture criterion is shown as the horizontal dashed red line.*

The relative consistency of failure times improved, with less than 0.5 hr differences between the 120 – 150 mm samples. It must be noted that sample fracture in the previous experiment was much more apparent due to the sudden drop in recorded force; however, this experiment revealed a gradual decrease in force, thus in this case a sample was considered fractured once the normalized force reached 10% of

its initial value. Both longer samples (160 and 170 mm) appeared to completely fail approximately 1 hr following the 150 mm sample, which provided a good visual distinction for showing the effects of sample length. The separation between the 120-150 mm vs the 160 and 170 mm samples was thought to occur due to a critical stress being achieved with the shorter samples which accelerated the slow crack growth phenomenon, however no major difference in fracture time occurred when varying sample length between 120 – 150 mm.

To try and explain the difference in fracture type between the first and second plaque tested, DSC analysis was performed on each 120 mm sample to reveal a crystallinity difference of approximately 9% (66% for the first plaque and 57% for the second). Such a difference in crystallinity could arise from processing conditions during the compression molding procedure, which provides evidence to how sensitive evaluating ESCR could be where consistency needs to be assured not only for testing conditions, but also sample creation. Considering how the bending and notching had been completed manually for these preliminary tests, and others have shown the variability that both operations could have on the failure time of a sample, it was decided to improve the force based testing procedure to ensure repeatable ESCR values could be obtained [39].

Designed Equipment

Priority was placed on designing a simple mechanism that could reproducibly notch a sample and bend a sample to eliminate inconsistencies from performing these operations manually. The Bell Test has two separate devices to accomplishing this, first the fodder chopper style (Figure 1-A) notcher creates a defect length-wise along the flat sample surface. Next, the sample is placed into a movable channel that when clamped together bend/loads the sample with the stress required to initiate environmental stress cracking. Considering the inefficiencies noted by others with this style of notcher and the two-step system

in general, it was decided to design a device that *combines both the notching and bending procedure into one step.*

After several iterations, the final design can be seen below in Figure 30 where a sample can be formed in a bending die with a 15.9 mm (5/8'') radius of curvature. A detailed engineering drawing is also provided in the Appendix.

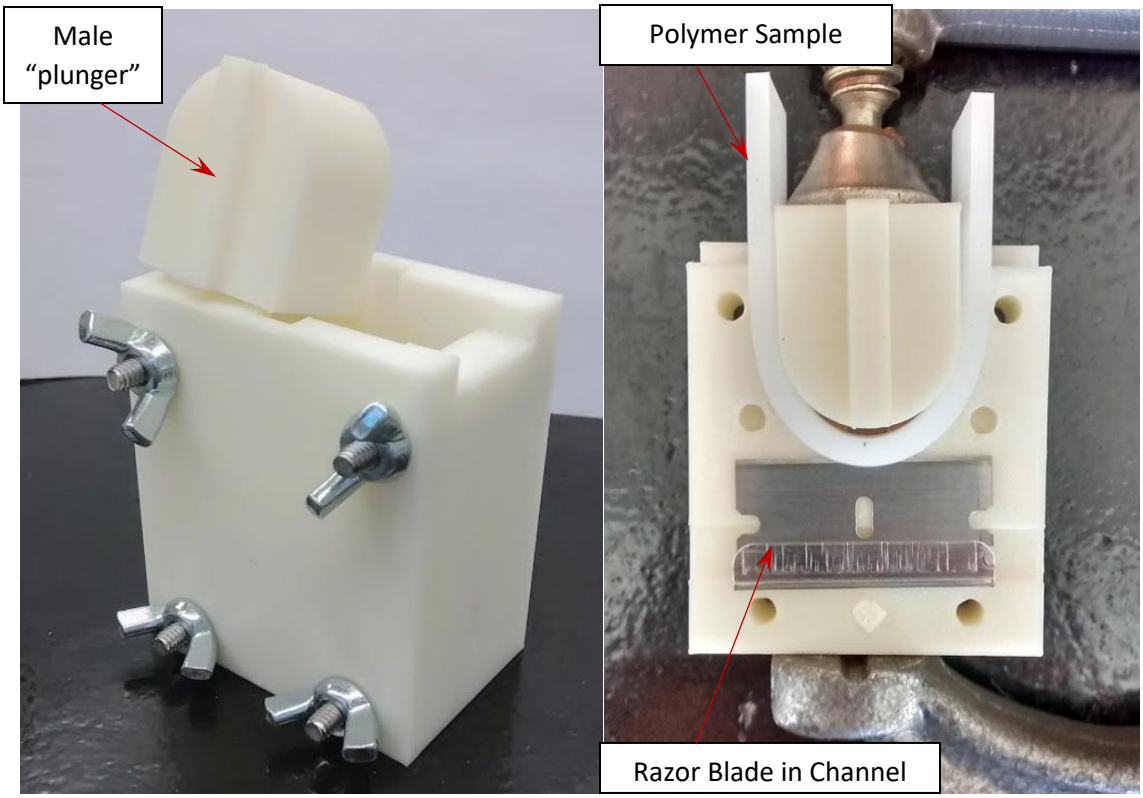

***Figure 30**: Notching and bending device. A photo of the assembled unit is shown to the left with the male plunger highlighted whereas a cross-section is shown on the right with bent sample and razor blade in place.*

The device was designed in two halves to provide easy placement of a razor blade into the blade channel depicted in Figure 30. With a blade fitted (No. 9 single edge industrial razor blade [purchased from the VWR Corporation], which is less obscure to find as the blades for the Bell Test), the halves can be press-fit together with the three centering pins lining the halves together. Four 44.5 mm (1 ¾'') number 6 screws with wing nuts are used to fully fasten the device together, which effectively clamps the razor blade in place, ensuring it does not move during use. Notch depth with this device is not

uniform due to the notching procedure occurring on a bent sample. The deepest point of the notch occurs at the apex of the curved sample and equates to a notch depth of roughly 0.5-0.65 mm to correspond to the ASTM D1693 standard.

The center line of a 115 mm long sample can then be marked and aligned within the channel at the top of the device. With everything in place, the male plunger is placed within its guides and the sample can slowly be bent and notched by pressing down on the plunger. Typically this procedure can be started by hand, but a c-clamp should be used to perform the final notching portion as high force is needed to seat the plunger. After bending, the c-clamp can be removed and the sample retained in an acrylic holder which houses the OMEGA sensor (Figure 31) that now reads forces compressively opposed to the tensile methods seen previously.

***Figure 31**: Acrylic sample retaining device with fitted OMEGA sensor to read forces in a compressive manner.*

The whole assembly can then be placed over a pre-heated bath of ageing fluid maintained at a constant 50°C; an IKA RET Basic hot plate and an ETA-D4 Fuzzy controller was used for the experiments. Data acquisition can then begin to gather the force response of the strained sample. Sampling rates were found to work best at approximately 1 Hz to balance profile resolution with data file size due to testing times.

Effects of Ageing Fluid on Sample Failure Time

Grade 1

With a reliable method of sample preparation created, a study was conducted utilizing resin Grades 1, 4, and 7 aged in fluids of full strength Igepal, a 10% solution of Igepal in de-ionized water, B100 biodiesel and 50°C air. Polymer resins covering a wide range of ESCR values (3 hr – 370 hr) were chosen to determine if force monitoring could detect unique sample behaviour upon exposure to a multitude of environments. Experiments were performed in triplicates and razor blades were refreshed after every fifth notch to reduce error, following Choi et al's findings [39]. The normalized force profile curves for Grade 1 can be seen below in Figure 32.

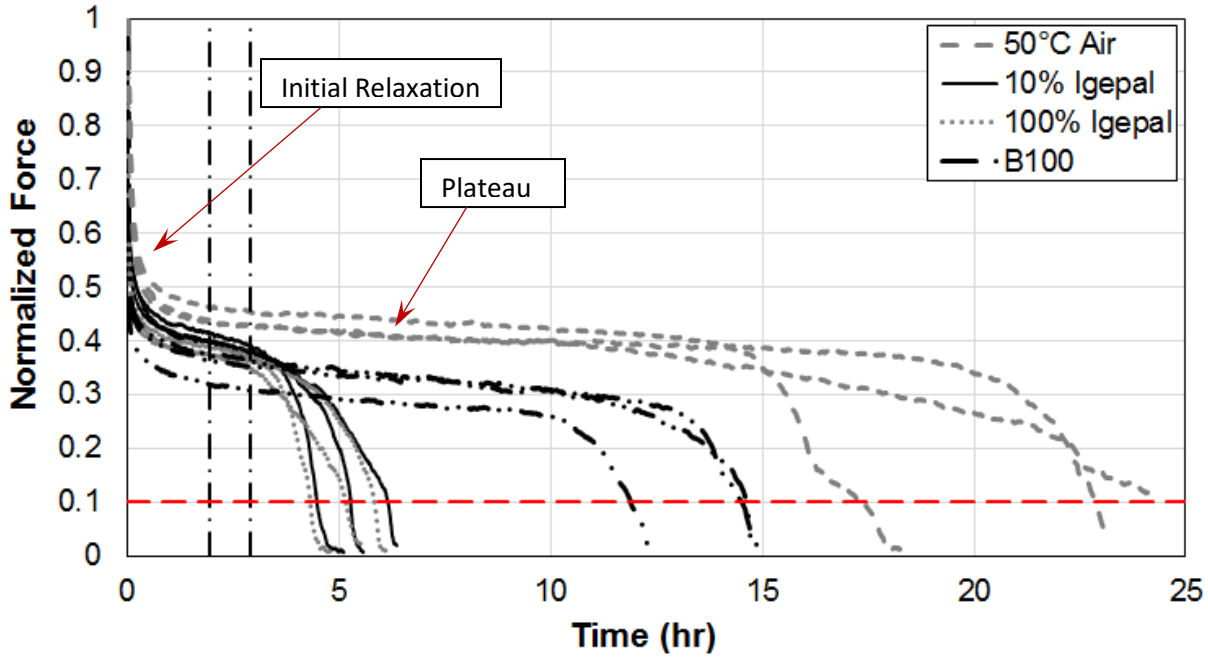

***Figure 32**: Force profiling curves for Grade 1 resin aged in 100% and 10% Igepal, B100 biodiesel and air. Dashed vertical lines at 1.9 hr and 2.9 hr represent when a separate sample of Grade 1 was removed and imaged. Fracture criterion is shown as the horizontal dashed red line. Peak loadings never exceeded ~30 N.*

Perhaps the most interesting observation of the profiles is the separation in failure time between ageing fluids, with Igepal samples failing first after approximately 5 hr, followed by biodiesel at 12.5 - 15 hr and finally the air aged samples at 17.5 - 25 hr. The differences in failure times seem to reflect the aggressiveness of the ageing fluid, with Igepal being ranked the most and air being ranked the least.

Biodiesel falling between the extremes suggested that it could be classified as an active environment, an important discovery.

Differences in the initial relaxation behaviour should also be noted, with the Igepal and biodiesel solutions provoking a 5%-10% greater reduction in normalized force compared to air before plateauing, which could indicate their plasticizing ability. Biodiesel's potential to partially plasticize Grade 1 was studied and confirmed in the Active Acoustics Chapter, while Igepal was not found to be capable of doing so in a static environment. The larger force reduction seen in Igepal aged samples compared to air could be explained by the added stress of the testing technique. Hittmair and Ullman were able to show imposed force/stresses could increase the solubility of a fluid within a polymer, which as a result will induce a larger plasticizing response [24]. Lustuger et al. also noted Igepal's ability to induce plasticization in a stressed environment and traced the fluids aggressiveness to its ability to diffuse into the amorphous (interlamellar) region of a polymer [42].

Unusually no differences could be seen between the 100% and 10% concentrations of Igepal used, which may be due to the polymer's lower molecular weight (High MFI – 8.8) and high crystalline properties. The low molecular weight reduces the probability of successful tie molecule/chain entanglement formation, reducing the ESCR of the polymer. A high crystallinity provides stiffness, which when bent and constrained, induces a large load. The combination of a low tie molecule concentration and high load would provoke an acceleration in ESC, which perhaps masks the Igepal concentration effects (i.e. failure rate is too rapid).

A separate sample of Grade 1 was also aged in a 10% Igepal solution and removed at select time points (shown in Figure 32 as vertical dashed lines) with the intention of linking the observations of the force profiling with crack progression. A selection of microscopy photos depicting the sample apex, striation phenomenon and the notch tip are presented below in Figure 33.

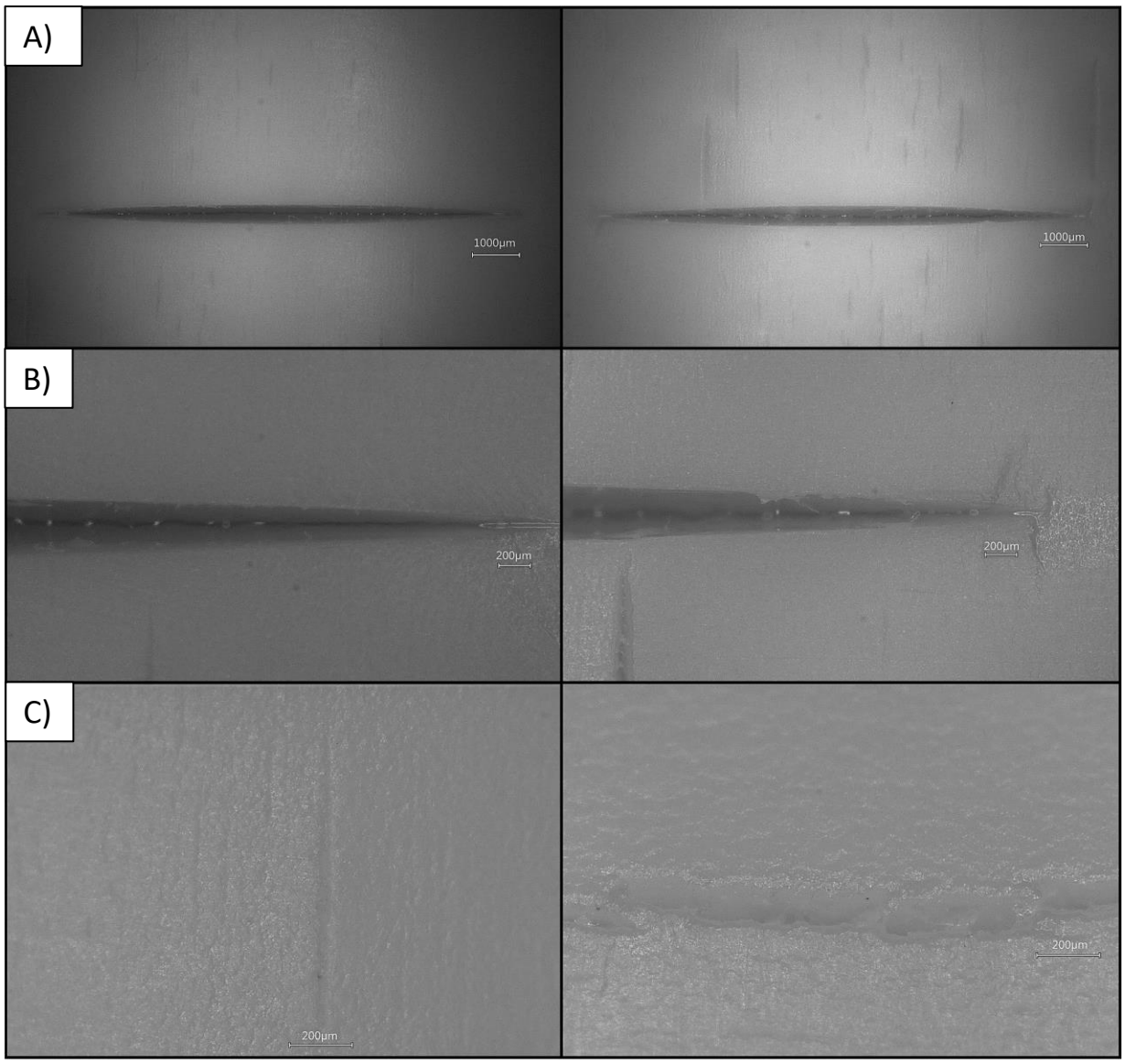

***Figure 33**: Images of Grade 1 resin after ageing in a 10% solution of Igepal in water for 1.9 hr. (Images on left) and 2.9 hr. (Images on right). A) Sample apex B) Notch Tip C) Striation formation*

Photos A and B of Figure 33 provide the best depiction of crack progression, which followed the decreasing forces recorded. As the sample ages in a strained configuration, stressed regions swell with Igepal, which causes the material to plasticize and further enhance localized stress. Micro voids form as entangled cilia begin to unravel, stressing the tie molecules which link lamella together. As the stress loading grows too large, tie molecules break and pull away from their respective crystalline bases and a craze forms. Crazes propagate and open with time to form cracks and in extreme cases, as seen with

Grade 1, form striation-like deformities (Figure 33-C). The contribution of this uncontrollable phenomenon leads to complete material failure with a brittle fracture.

When looking at the fracture area of each sample, an excellent visual distinction can be seen which supports the force profiles shown previously. Figure 34 below compares the fracture areas seen after ageing in a solution of 10% Igepal in water, B100 biodiesel and 50°C air.

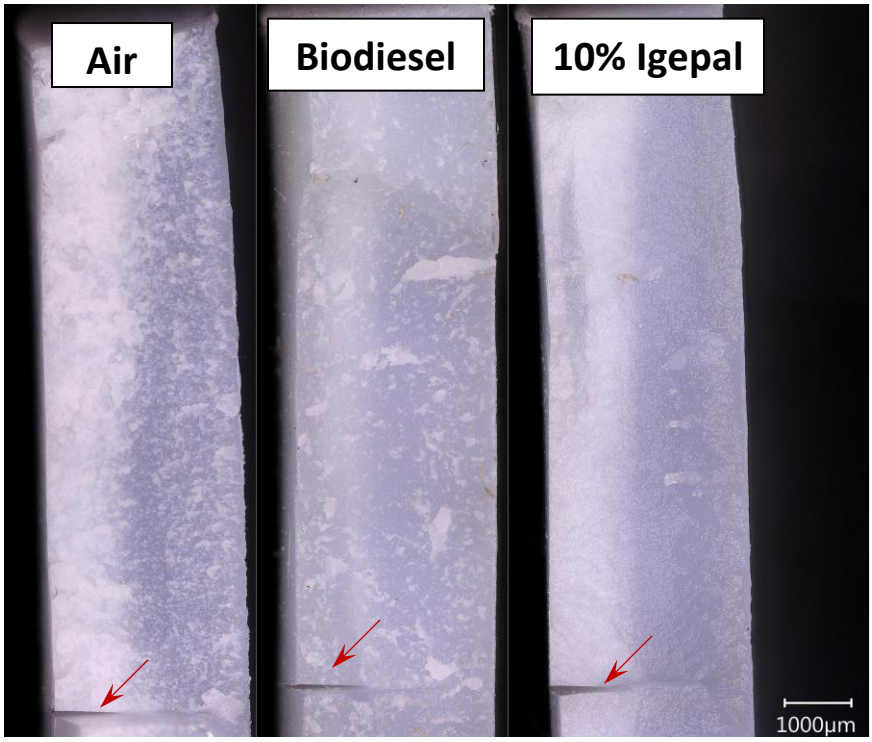

***Figure 34**: Newly formed fracture surface of Grade 1 polymer after ageing in Air, Biodiesel and 10% Igepal. The notch tip is identified for each sample with a red arrow. The fracture surface naturally progresses width-wise across the sample, perpendicular to the notch*

The fracture area of the air aged sample appears fibrous and rough, indicating a drawn out failure process, where crystal lamella become bent/stretched and the load bearing tie molecules pull out from their respective lamella or fracture. The biodiesel aged sample shows some of the same signatures as the air aged sample, however the surface overall appears much smoother which suggests an environmental stress cracking type failure. Surface texture of the Igepal aged sample shows almost no signs of fibrillation; a very brittle type failure is evident with Igepal which corresponds to the assisted disentanglement of interlamellar linkages by the presence of the active environment. It is very intriguing to see the biodiesel

producing a fracture surface similar to that of Igepal, it may not have the same aggressiveness as Igepal, but this observation further provides evidence to its active nature.

Force Profiling Curve Analysis

It was thought that important features of the force curves could be used to assist in quantifying the ESCR properties of the polymer resins. The simplest parameter to examine would be the absolute failure time of a sample, which noted previously was determined to be when the force value fell below 10% of the maximum recorded force. A summary of the failure times of Grade 1 is presented below in Table 2.

***Table 2**: Average failure time of Grade 1 after exposure to varying environments. Error in failure time reflects the standard error of three trials.*

Ageing Environment	Average Failure Time (hr)
50°C Air	21.5 ± 2.1
10% Igepal	5.3 ± 0.5
100% Igepal	5.1 ± 0.4
B100 biodiesel	13.6 ± 0.9

The values in Table 2 reflect the rather high variation seen in with this visual based technique, however distinguishing between the three main ageing environments (air, Igepal, biodiesel) is readily apparent. To try and improve predicting ESCR, and perhaps shorten the testing time, the onset of failure was thought to be a better metric comped to its visual counterpart. The onset of failure was found by examining the region of the curve where the plateau transitioned to a negative sloping arc. To quantify the time the transition began, a cubic regression was performed on the curve which included approximately the latter half of the plateau area and the complete failure region. The second derivative was taken of the regressed function and the resulting inflection point was used to identify failure onset. A summary of failure onset times is presented below in Table 3.

***Table 3**: Average failure onset time of Grade 1 after exposure to varying environments. Error in failure time reflects the standard error of three trials.*

Ageing Environment	Average Failure Onset Time (hr)
50°C Air	N/A
10% Igepal	2.5 ± 0.1
100% Igepal	2.2 ± 0.4
B100 biodiesel	9.2 ± 0.3

Using the curve fitting method seems to produce smaller error for most environments; however, no difference in onset time could be seen between the 10% and 100% concentrations. The failure onset time also better reflects the published 3 hr ESCR value of Grade 1 compared to the found 2.5 hr. The onset time for air aged samples were not computed due to the sporadic nature of the forces recoded during the trials.

Grade 7

The force profiles generated for Grade 7 resin can be seen below in Figure 35 with comparable trends to Grade 1 (Figure 32), however important differences also exist.

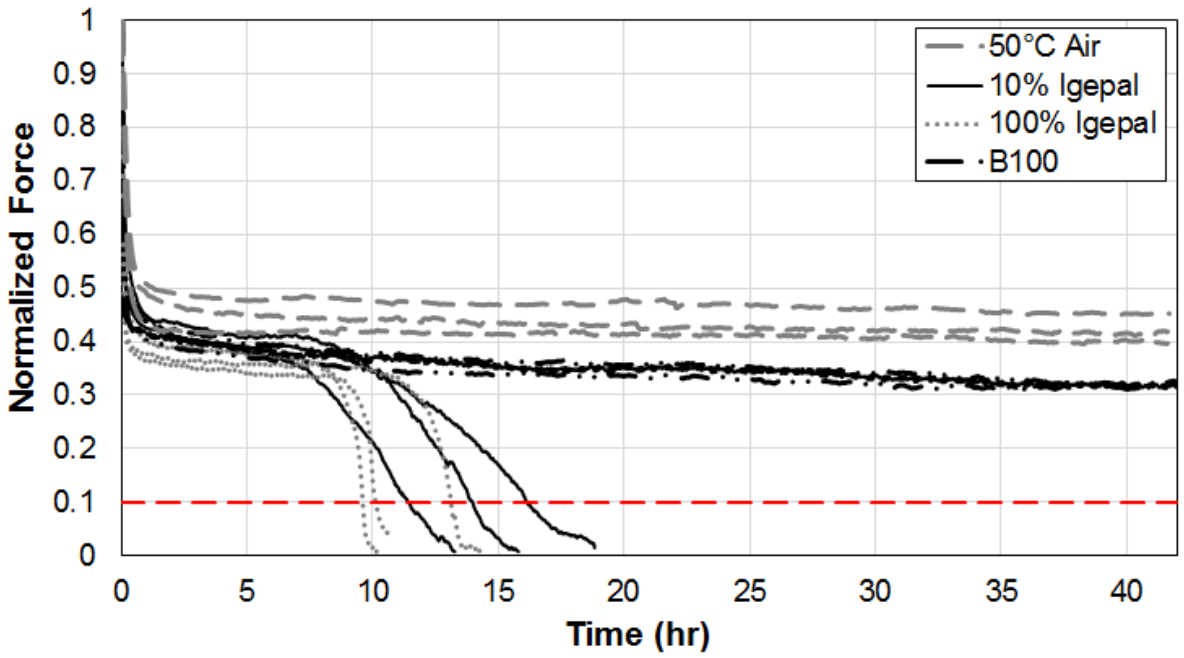

***Figure 35**: Grade 7 force profiling after ageing in 100% and 10% Igepal, B100 biodiesel and 50°C air. Fracture criterion is shown as the horizontal dashed red line*

Again, plasticization for both Igepal and biodiesel aged samples is seen through the initial relaxation, which agrees with previous observations. A grouping of fracture times for the Igepal aged samples was seen to span 10 hr – 20 hr and visual differences are apparent in the rate of failure between the concentrations. The steeper rate of load decay for the 100% Igepal solution is unusual as aggressiveness has been shown to be higher in 10% solutions [21, 22]. Fracture rate discrepancies could be explained as the previously cited studies used different testing configurations; one used a tensile type loading system similar to ASTM D5397, while the other constructed a custom four-point bending apparatus. Regardless of the testing configuration used, it could be beneficial to investigate a range of Igepal concentration points to see if other fracture behaviour occurs.

The lack of fracture for the biodiesel sample was rather unfortunate as tests were stopped after approximately 42 hr so keep testing times to a minimum. One biodiesel trial was run extra-long for 116 hr to see how the force profiling progressed. The notch tip of the 116 hr aged sample can be seen in Figure 36, where no indications of crack initiation/progress are apparent however the notch itself appears wider compared to a freshly notched sample. The force profile also revealed a continuous plateau region, which could indicate one of two things; the systems inability to detect internal structural damage, or the lack of damage altogether.

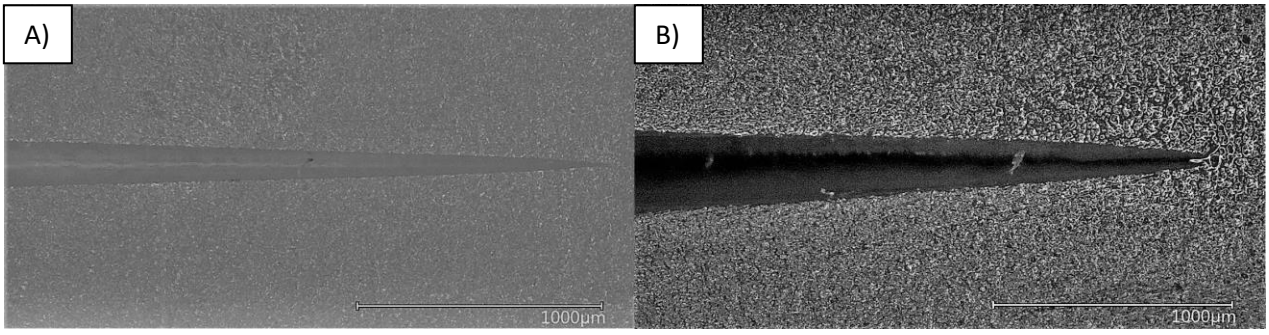

***Figure 36**: Notch tip of a G7 sample pre-ageing (A) and after aged in Biodiesel for 116 hr (B).*

Considering the radius of curvature (15.9 mm) of a bent sample in a force profiling test is significantly smaller compared to the Bell Test (5.1 mm), the loads that a sample endures would be less,

which could explain the lack of any stress cracking behaviour seen with the biodiesel aged samples. It is unknown how long it would take to witness the onset of failure for a biodiesel aged sample, which could pose a problem for longer rated ESCR materials.

Force Profiling Curve Analysis

The average failure times for the fractured specimens (10% & 100% Igepal) are presented below in Table 4, where a slight difference can be seen between the two concentrations.

***Table 4**: Average failure time of Grade 7 after exposure to varying environments. Error in failure time reflects standard error of three trials.*

Ageing Environment	Average Failure Time (hr)
10% Igepal	13.8 ± 1.4
100% Igepal	10.9 ± 1.1

Interestingly, the failure times found are less than those reported by the resin manufacturer (20 hr). It was expected that the failure times of the force profiling test should be the same, if not longer compared to the Bell Test due to the lower stresses of the larger bent sample. The most likely explanation for this observation could be the different sample processing/molding conditions, as this was directly witnessed previously in the Effects of Sample Length on Failure Time Chapter when testing Grade 2 resin. The computed failure onset times also presented below in Table 5.

***Table 5**: Average failure onset time of Grade 7 after exposure to varying environments. Error in failure time reflects standard error of three trials.*

Ageing Environment	Average Failure Onset Time (hr)
10% Igepal	4.4 ± 0.6
100% Igepal	6.1 ± 0.6

Using the same cubic regression technique discussed earlier, the onset time is much earlier (4.4 hr ± 0.6 hr for 10% Igepal, 6.1 hr ± 0.6 hr for 100% Igepal) compared to the complete failure time (13.8 hr ± 1.4 hr for 10% Igepal, 10.9 hr ± 1.1 hr for 100% Igepal), which appears to appropriately be represented when looking back at Figure 35. This really demonstrates the potential for analysis of force profiling as

onset of failure times could better communicate ESCR rankings by distinguishing between samples with abrupt failure signatures vs. others with long, drawn out profiles.

Grade 4

The lack of a fracture for Grade 7 aged in biodiesel was noted to be of concern as higher rated ESCR materials would probably fail to produce any significant force related activity. This proved to be correct as only the plateau region was seen when ageing Grade 4 across all fluids for a maximum time of 42 hours (Figure 37). Only one polymer sample of Grade 4 was aged in each fluid due to the time devotion needed and only being able to monitor one sample at a time.

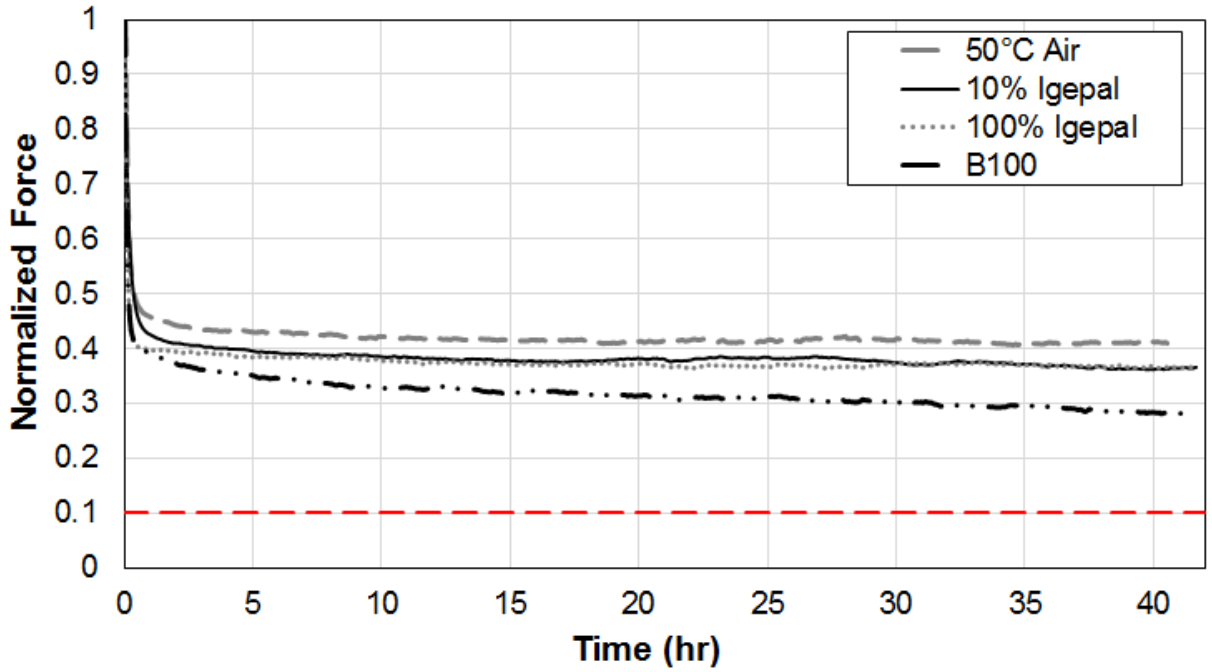

***Figure 37**: Grade 4 force profiling showing only, the initial relaxation and plateau region after 42 hours of ageing. Fracture criterion is shown as the horizontal dashed red line*

The plasticizing ability of biodiesel and Igepal are clearly seen again though the force profiling, however a smaller response for Igepal is seen when compared against the previously tested grades. The smaller plasticizing response may be due to the higher ESCR value of this material, reflected by the strain hardening ability (Figure A2 in Appendix A) and its bimodal nature preventing Igepal from diffusing/swelling the material.

Despite no immediate fractures being visible after testing the samples, observation of both the Igepal aged samples (10% & 100%) after an undefined period of time in a relaxed state at room temperature revealed the development of cracking at the notch tips which is highlighted in Figure 38. Unusually, no fracture indications were seen with the biodiesel aged sample, even after an extended period of time despite its ability to better plasticize the material compared to Igepal (Figure 37).

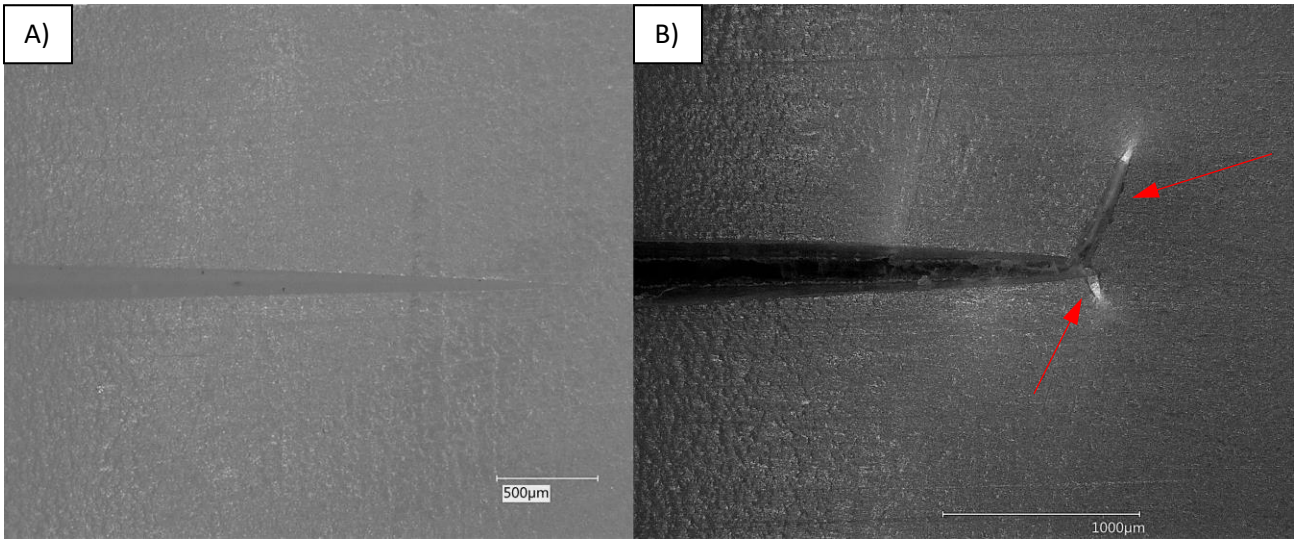

***Figure 38**: Excellent example of environmental stress cracking occurring at the notch tip after an undefined period of ageing. A fresh notch (A) is compared against the aged sample (B).*

The evidence of cracking post-exposure to Igepal implies the testing configuration is able to induce stress cracking behaviour in high ranking ESCR materials, therefore it should be possible to quantify this with force profiling. Possible improvements to the current set-up for easier detection of ESC is discussed further in the Future Recommendation Chapter.

Conclusions

A novel force based measuring technique was created to improve upon the widely used Bell Test for evaluating ESCR. The created system borrowed many aspects of the Bell Test (bent sample, notching) to keep testing simplistic, and attempted to refine sample preparation with a created device designed to combined sample notching and bending.

Collected force profiles provided a unique look at how ESCR progresses where three distinct regions of sample embrittlement where witnessed; the initial relaxation marked by sample plasticization, a plateauing of force signifying a relative steady state and the onset of sample failure where recorded force falls indicating crack propagation and ultimately material failure. Analysis of the force curves through cubic regression to find the inflection point proved to be one method of identifying the onset of failure, an important feature for defining ESCR rankings and a tool which could reduce testing times.

Various ageing environments were also examined where it was discovered biodiesel could accelerate sample failure while in a stressed environment. Supplementary images of the fracture zone of a biodiesel aged sample showed significant similarities to an Igepal accelerated fracture, further proving its stress crack capabilities.

Overall, force profiling is a promising alternative for investigating resin ESCR and future work will be performed to improve on this emerging analysis technique.

Evaluation of Biodiesel as an Environmental Stress Cracking Agent

Introduction

A common parameter among most ESCR testing procedures is the detergent Igepal CO630 due to its ability to accelerate failure times in otherwise environmentally stable polymers. DeCoste et al. were the first to standardize the use of Igepal as a stress cracking agent after investigating a variety of fluids to determine environmental activity; a summary of their findings can be seen below in Table 6 [2].

***Table 6**: Environmental stress cracking agents identified through use of the Bell Test. Table adapted from [6].*

EFFECT OF VARIOUS MATERIALS ON 55 GRADE POLYETHYLENE

(Crack resistance test)

Active Environments	
Aliphatic and aromatic liquid hydrocarbons	Metallic soaps
Alcohols	Sulfated and sulfonated alcohols
Organic acids	Alkanolamines
Ester-type plasticizers	Polyglycol ethers
Vegetable oils	Sodium and potassium hydroxide
Animal oils	Depolymerized rubbers
Mineral oils	Polybutenes
	Silicone fluids

Inactive Environments	
Water	Rosin
Polyhydric alcohols	Selected asphalts
Sugars	Paraffin wax
Selected saponins	Bentonite
Hydrolyzed protein	Acid and neutral inorganic salts

An interesting observation is the identification of both ester-type plasticizers and vegetable/animal oils as being environmentally active as these agents are structurally similar to biodiesel, a common substitute for petroleum diesel in the automotive industry. Straight vegetable oil can be used directly as fuel; however, the lower viscosity and potential to solidify at lower temperatures has prevented it from being widely adopted [43]. Alternatively, biodiesel produced from either vegetable or animal oils has been a fierce competitor in the renewable energy sector due to better flow characteristics; however, problems still exist at temperatures common to northern climate winters [44]. To remedy some of the

cold flow properties to make biodiesel a viable, lower emission alternative fuel, it is commonly blended with petroleum based diesel.

In Ontario Canada, government mandates have been issued stating that by 2017 4% of the total volume of diesel sold must be bio-based and the blended fuel must comply with the Canadian General Standard Board's quality standards [45]. Since many of the engine performance issues associated with biodiesel has been remedied though blending and better production practices, the possibility of biodiesel potentially being an environmental stress cracking agent seems to be an overlooked threat. As use of polymers as fuel tanks and engine components are becoming increasingly common, careful attention needs to be taken to ensure the lifetime of said components are not compromised with fuel bending technology. Work by Thompson at al. [46] and Richaud et al. [47] studied the effects of biodiesel on polyethylene in a static environment (no force application), where both concluded that no major degradation could be seen after lengthy exposure times.

As discussed in the Literature Review, common fluids in contact with polyethylene under no stress could quickly turn aggressive and accelerate cracking if minor forces are imposed on the material. The following chapter acts as an extension to the force profiling section to verify the possibility of biodiesel being an active ESC agent of polyethylene through use of the Bell Test.

Testing and Results

Preliminary testing of biodiesel in an ESCR setting was completed using the small tank set-up described in the Passive Acoustics Chapter (Figure 14) with Grade 1 resin. Ageing took place in both B100 biodiesel and a solution of 10% biodiesel in de-ionized water. A lower concentration of biodiesel was tested as work by Qian et al. determined that full strength solutions may not be the most aggressive stress cracking fluid [21]. Traditionally, a 10% solution of Igepal with water is used in the Bell Test, and this configuration was chosen with biodiesel as a starting point. After active video monitoring, fractures were

visible in the B100 and 10% biodiesel/water solution after 2.5 and 3 hours indicating biodiesel could be a stress cracking agent.

Examination of the fractured samples also showed rather interesting results with distinct staining of the sample around the facture area, as evident in Figure 39 below.

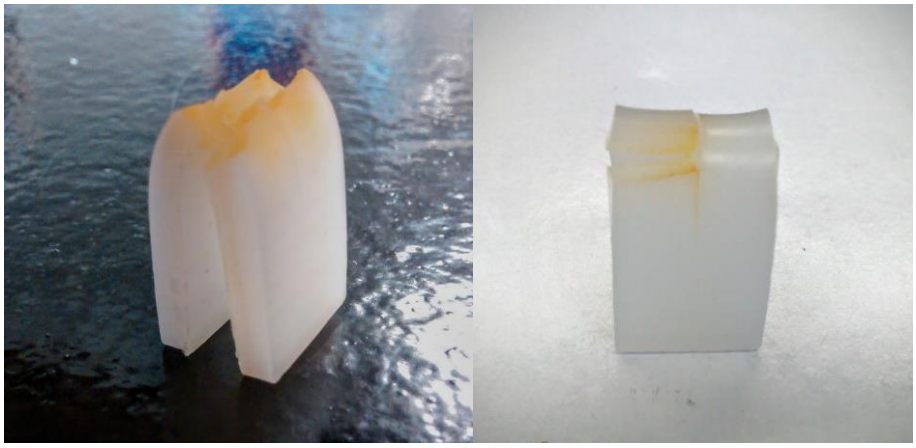

Figure 39: *Staining of the fracture area by biodiesel on a sample of Grade 1 polyethylene.*

Gentle washing of the samples with a water spray bottle after testing was unable to fully remove the signs of biodiesel. Investigating the mechanisms behind this staining phenomenon may open further opportunities to study ESC with focus on the staining action of different stress cracking agents, and possibly developing this observation into a detection technique for ranking the ESCR of materials.

Regarding the initial discovery of biodiesel being a potential stress cracking agent, a large scale ESCR trial utilizing the Bell Test was organized using 8 samples of Grades 1, 4, 5, 6, and 7 for analysis. Since a 10% biodiesel/water solution was found to give similar failure times as B100 biodiesel, the 10% solution was used during the tests. A blend of B10 biodiesel (10% biodiesel in petroleum based diesel) was also tested to model an actual solution in a commercial diesel tank. Repeat trials were completed for Grades 4, 5, 6 and 7, results from the preliminary small scale test were deemed sufficient as repeats for Grade 1. Observations of the samples were made at least once per working day, and agitation (shaking) of the fluid was done regularly to minimize separation of biodiesel in the water solution

A summary of the results can be seen in Table 7, with ESCR being represented in typical F_{50} fashion

***Table 7**: Determined ESCR values for polyethylene resins aged in a solution of 10% biodiesel in water or 10% biodiesel in petroleum based diesel.*

Resin Grade	ESCR F_{50} hours			
	10% Biodiesel in Water		10% Biodiesel in Diesel	
	Trial 1	Trial 2	Trial 1	Trial 2
1	2	<2	2	<2
4	>1000	787	>1000	885
5	>1000	>1000	>1000	>1000
6	>1000	>1000	>1000	>1000
7	166	187	166	187

A rather interesting result is the acceleration in failure times both biodiesel solutions cause for Grades 4 and 7. Based these observations and what was witnessed in the force profiling section, it was concluded ***that biodiesel can be classified as an environmental stress cracking fluid***. Apart from Grades 4 and 7 being susceptible to biodiesel, one sample of Grade 5/9 was also seen to fail on the final observation in the 10% biodiesel/water solution, indicating biodiesel may enhance stress cracking in this material too. Grade 6 (LLDPE) was not seen to show any signs of crazing/cracks, proving its superior ESCR compared to the other high density materials. At the completion of each trial, more fractures were seen in the biodiesel/water solution, but it is unknown if this solution is more aggressive compared to the B10 blend. Fractures were also more apparent in the repeat trials and can be explained as more frequent agitation was implemented.

Conclusions

The stress cracking capability of biodiesel was examined by conducting a Bell Test on five grades of polyethylene aged in solutions of 10% biodiesel in water or 10% biodiesel in petroleum based diesel. Samples of Grade 1, 4 and 7 resin were seen to fracture before the stopping point of 1000 hours proving biodiesels nature to accelerate cracking in a stressed environment. Unique yellow staining was also seen on fractured samples which should be examined further to better understand the mechanism behind environmental stress cracking.

Final Conclusions

Environmental stress cracking has been a problem in the plastics industry for over 70 years, affecting a range of polymers from semi-crystalline polyolefins to glassy polycarbonates. Various mechanisms of action have been proposed to describe the ESC phenomenon, with most agreeing that a stressed polymer in contact with an active environment will readily plasticize and compromise key interlamellar linkages, leading to brittle failure. Advancements in polymer formulation such as additional short chain branching and large molecular weights have vastly improved environmental stress cracking resistance for materials in the harshest of environments. Despite the progress made in creating high performing ESCR materials, very little has been done for improving the actual evaluation techniques for testing the materials.

The work presented outlines a variety of novel techniques to evaluate the ESCR of polyethylene. It was found that while initially promising, passive acoustics could not be used as a failure detection system due to the low amplitude nature of the events associated with slow crack growth progression. The environment itself was also found to be extremely noisy and the highly attenuative properties of polymers quickly curtailed any possibility of signal detection. Alternatively, active acoustics were tested to see if probing the material with ultrasonic waves could infer ESCR properties. The plasticizing ability of both toluene and biodiesel could be detected by ultrasonic velocity measurements, however no indication of a material's ESCR could be deduced. Due to the complexity of using acoustics or ultrasonics as a diagnostic technique, this method of evaluation was retired in favour of a novel force profiling system.

A custom device was created that combined the notching and bending procedures of the Bell Test and a special fixture fitted with a load cell to monitor the response that a polymer had to being bent and strained. It was found that force profiling could provide valuable insight into the progression of slow crack growth by mapping the relaxation and eventual environmentally assisted failure of polymers. Through

this technique and additional work following ASTM D1693, it was found the biodiesel can be classified as an active environment, an important finding for application of polymers in fuel related settings.

Recommendations for Future Work

Force profiling seems to have high potential for evaluating ESCR properties of polymers and to improve on the technique, the designed bending/notching device should be tweaked to smooth the ergonomics of the procedure. The current method relies on initially bending the polymer sample by hand and finishing with a c-clamp; this could be improved by implementing a lever based system so only one fluid motion would be needed to prep the sample.

As mentioned previously, cracking of Grade 4 & 7 resins were not seen within a reasonable period of time when biodiesel was used as an ageing fluid. It was believed the bending stresses were too low to provoke an ESC response. To remedy the low stresses, a tighter bend radius could be implemented or a more sensitive load cell could also be tested (5 kg force instated of the 10 kg force used). For testing on a larger scale (more than one sample at a time) strain gauges could be placed on a custom designed sample retaining device whose deformation could be measured to inferentially monitor the polymer failure profile. (A strain gauge is approximately 3 times cheaper than an equivalent load cell).

The analysis technique of performing a cubic regression proved to be a rather simple method of determining the onset failure time and may not be the best approach due to the unusual failure profiles that could occur (Grade 1 aged in air) making the regression inaccurate. Different analysis techniques should be investigated in the future, possibly based on changes in the plateau region, so analysis could be performed in conjunction with an ESCR test to potentially shorten testing times.

The use of load cells opens many alternative testing configurations, with an example of a compressed pipe section seen below in Figure 37.

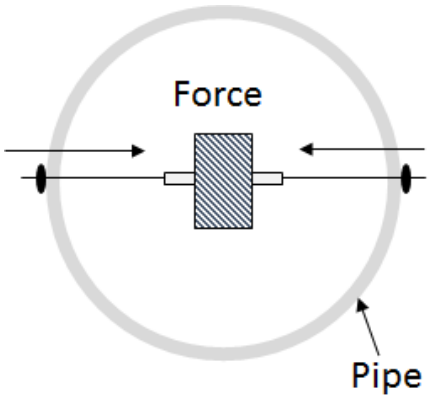

***Figure 40**: Alternative ESCR testing configuration where a compressed pipe could be submerged in a heated bath to monitor force loading.*

Essentially a short section of pipe is cut and two holes drilled to allow threaded rod to pass though and attach to the load cell located in the middle of the pipe. Nuts could then be tightened to impose a compressive load on the pipe, which would be interpreted as a tensile force on the sensor. The load potential from this configuration would be more tunable compared to a bent strip set-up and loads could be significantly higher if desired.

References

1. Robeson, Lloyd M. "Environmental stress cracking: A review." *Polymer Engineering & Science* 53.3 (2013): 453-467.
2. DeCoste, J. B., F. S. Malm, and V. T. Wallder. "Cracking of Stressed Polyethylene." *Industrial & Engineering Chemistry* 43.1 (1951): 117-121.
3. ASTM International. *ASTM D1693-15 Standard Test Method for Environmental Stress-Cracking of Ethylene Plastics*. West Conshohocken, PA: ASTM International, 2015. Web. 31 Mar 2017.
4. ASTM International. *ASTM D5397-07(2012) Standard Test Method for Evaluation of Stress Crack Resistance of Polyolefin Geomembranes Using Notched Constant Tensile Load Test*. West Conshohocken, PA: ASTM International, 2012. Web. 31 Mar 2017.
5. Hsuan, Y. G., and R. M. Koerner. "The Single Point-Notched Constant Load Test: A Quality Control Test for Assessing Stress Crack Resistance." *Geosynthetics International* 2.5 (1995): 831-843.
6. ASTM International. *ASTM F1473-16 Standard Test Method for Notch Tensile Test to Measure the Resistance to Slow Crack Growth of Polyethylene Pipes and Resins*. West Conshohocken, PA: ASTM International, 2016. Web. 31 Mar 2017.
7. ISO 16770. *Plastics - Determination of environmental stress cracking (ESC) of polyethylene - Full-notch creep test (FNCT)*
8. Portnoy, Robert C. *Medical plastics: degradation resistance and failure analysis*. William Andrew, 1998.
9. Wright, David C. *Environmental stress cracking of plastics*. iSmithers Rapra Publishing, 1996.
10. Arnold, J. C. "Environmental stress crack initiation in glassy polymers." *Trends in polymer science* 4.12 (1996): 403-408.
11. Soares, João BP, R. F. Abbott, and J. D. Kim. "Environmental stress cracking resistance of polyethylene: The use of CRYSTAF and SEC to establish structure–property relationships." *Journal of Polymer Science Part B: Polymer Physics* 38.10 (2000): 1267-1275.
12. Al-Saidi, Lutfi F., Kell Mortensen, and Kristoffer Almdal. "Environmental stress cracking resistance. Behaviour of polycarbonate in different chemicals by determination of the time-dependence of stress at constant strains." *Polymer Degradation and Stability* 82.3 (2003): 451-461.
13. Bubeck, R. A., et al. "Environmental stress cracking in impact polystyrene." *Polymer Engineering & Science* 21.10 (1981): 624-633.
14. Kawaguchi, Takafumi, et al. "Environmental stress cracking of poly (acrylonitrile-butadiene-styrene)." *Polymer engineering and science* 39.2 (1999): 268.
15. Breen, J., and D. J. Van Dijk. "Environmental stress cracking of PVC: effects of natural gas with different amounts of benzene." *Journal of materials science* 26.19 (1991): 5212-5220.
16. Lustiger, A., and R. L. Markham. "Importance of tie molecules in preventing polyethylene fracture under long-term loading conditions." *Polymer* 24.12 (1983): 1647-1654.

17. Deblieck, Rudy AC, et al. "Failure mechanisms in polyolefines: The role of crazing, shear yielding and the entanglement network." *Polymer* 52.14 (2011): 2979-2990.
18. Lustiger, A., and R. D. Corneliussen. "The role of crazes in the crack growth of polyethylene." *Journal of materials Science* 22.7 (1987): 2470-2476.
19. Seguela, Roland. "Critical review of the molecular topology of semicrystalline polymers: The origin and assessment of intercrystalline tie molecules and chain entanglements." *Journal of Polymer Science Part B: Polymer Physics*43.14 (2005): 1729-1748.
20. Lustiger, A., and R. L. Markham. "Importance of tie molecules in preventing polyethylene fracture under long-term loading conditions." *Polymer* 24.12 (1983): 1647-1654.
21. Qian, R., X. Lu, and N. Brown. "The effect of concentration of an environmental stress cracking agent on slow crack growth in polyethylenes." *Polymer* 34.22 (1993): 4727-4731.
22. Rink, M., et al. "Effects of detergent on crack initiation and propagation in polyethylenes." *European Structural Integrity Society* 32 (2003): 103-114.
23. Ayyer, R., A. Hiltner, and E. Baer. "Effect of an environmental stress cracking agent on the mechanism of fatigue and creep in polyethylene." *Journal of materials science* 43.18 (2008): 6238-6253.
24. Hittmair, P., and Robert Ullman. "Environmental stress cracking of polyethylene." *Journal of Applied Polymer Science* 6.19 (1962): 1-14.
25. Brown, H. R. "A theory of the environmental stress cracking of polyethylene."*Polymer* 19.10 (1978): 1186-1188.
26. Ward, A. L., et al. "The mechanism of slow crack growth in polyethylene by an environmental stress cracking agent." *Polymer* 32.12 (1991): 2172-2178.
27. Boyd, Richard H. "Relaxation processes in crystalline polymers: molecular interpretation—a review." *Polymer* 26.8 (1985): 1123-1133.
28. Huang, Yan-Ling, and Norman Brown. "The effect of molecular weight on slow crack growth in linear polyethylene homopolymers." *Journal of materials science* 23.10 (1988): 3648-3655.
29. Huang, Yan - Ling, and Norman Brown. "The dependence of butyl branch density on slow crack growth in polyethylene: kinetics." *Journal of Polymer Science Part B: Polymer Physics* 28.11 (1990): 2007-2021.
30. Yeh, J. T., Jung - Horng Chen, and Huei - Song Hong. "Environmental stress cracking behavior of short - chain branch polyethylenes in Igepal solution under a constant load." *Journal of applied polymer science* 54.13 (1994): 2171-2186.
31. Cheng, Joy J., Maria A. Polak, and Alexander Penlidis. "Influence of micromolecular structure on environmental stress cracking resistance of high density polyethylene." *Tunnelling and Underground Space Technology* 26.4 (2011): 582-593.
32. Chen, Yang, et al. "Investigations of environmental stress cracking resistance of HDPE/UHMWPE and LDPE/UHMWPE blends." *Journal of Polymer Research* 20.5 (2013): 141

33. Wunderlich, Bernhard, and C. M. Cormier. "Heat of fusion of polyethylene." *Journal of Polymer Science Part A-2: Polymer Physics* 5.5 (1967): 987-988.
34. Yarysheva, Alena Yu, et al. "The structural evolution of high-density polyethylene during crazing in liquid medium." *European Polymer Journal* 66 (2015): 458-469.
35. Su, Zhongqing, Lin Ye, and Ye Lu. "Guided Lamb waves for identification of damage in composite structures: A review." *Journal of sound and vibration* 295.3 (2006): 753-780.BoilerFurnace
36. Hatanaka, Hiroaki, et al. "Ultrasonic creep damage detection by frequency analysis for boiler piping." *Journal of Pressure Vessel Technology* 129.4 (2007): 713-718.
37. Piche, L. "Ultrasonic velocity measurement for the determination of density in polyethylene." *Polymer Engineering & Science* 24.17 (1984): 1354-1358.
38. Gomes, F. P. C., et al. "Evaluating the influence of contacting fluids on polyethylene using acoustic emissions analysis." *Polymer Testing* 39 (2014): 61-69.
39. Choi, B-H., M. Cassiday, and P. Jimenez. "IMPROVEMENT OF THE TEST PROCEDURE OF AN ENVIRONMENTAL STRESS CRACKING RESISTANCE TEST OF HIGH-DENSITY POLYETHYLENE." *Experimental Techniques* 33.4 (2009): 43-51.
40. Jar, P-Y. Ben. "Measurement of Environmental Stress Cracking Resistance (ESCR) Using Notch-Free Specimens." *ASME 2015 Pressure Vessels and Piping Conference*. American Society of Mechanical Engineers, 2015.
41. Jar, Ben, and Yi Zhang. "Evaluation of a New Approach for Characterizing Environmental Stress Cracking Resistance (ESCR) of Polyethylene." *ASME 2016 Pressure Vessels and Piping Conference*. American Society of Mechanical Engineers, 2016.
42. Lustiger, A., and R. D. Corneliussen. "Environmental stress crack growth in high-density polyethylene." *Journal of Polymer Science Part C: Polymer Letters* 17.5 (1979): 269-275.
43. Nwafor, O. M. I. "The effect of elevated fuel inlet temperature on performance of diesel engine running on neat vegetable oil at constant speed conditions." *Renewable energy* 28.2 (2003): 171-181.
44. Knothe, Gerhard. "Improving biodiesel fuel properties by modifying fatty ester composition." *Energy & Environmental Science* 2.7 (2009): 759-766.
45. Murray, G. "Greener Diesel Regulation." *Ontario.ca*. Ministry of the Environment and Climate Change, 30 Mar. 2017. Web. 12 Apr. 2017.
46. Thompson, M. R., et al. "Long term storage of biodiesel/petrol diesel blends in polyethylene fuel tanks." *Fuel* 108 (2013): 771-779.
47. Richaud, Emmanuel, Bruno Flaconnèche, and Jacques Verdu. "Biodiesel permeability in polyethylene." *Polymer Testing* 31.8 (2012): 1070-1076.

Appendix A – Supplementary Figures

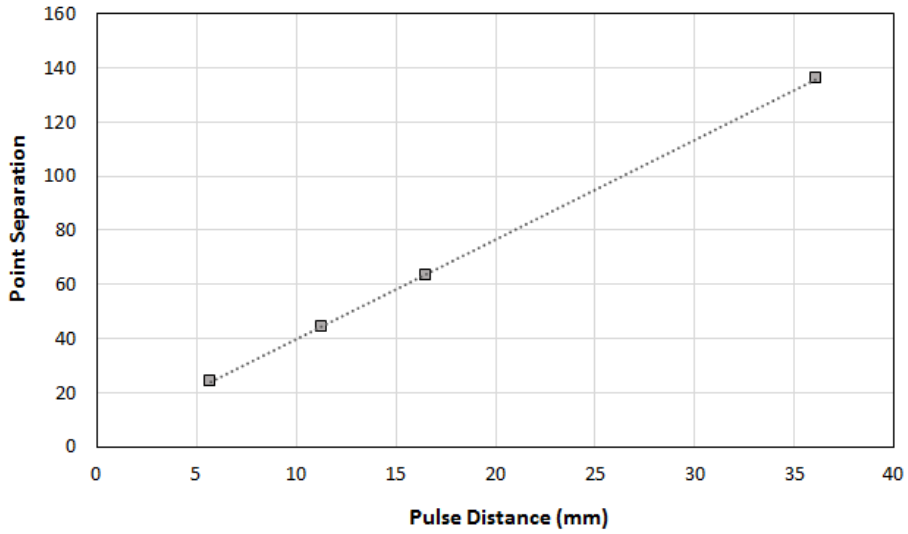

***Figure A-1**: Calibration curve created for ultrasonic testing with varying thicknesses of HDPE material.*

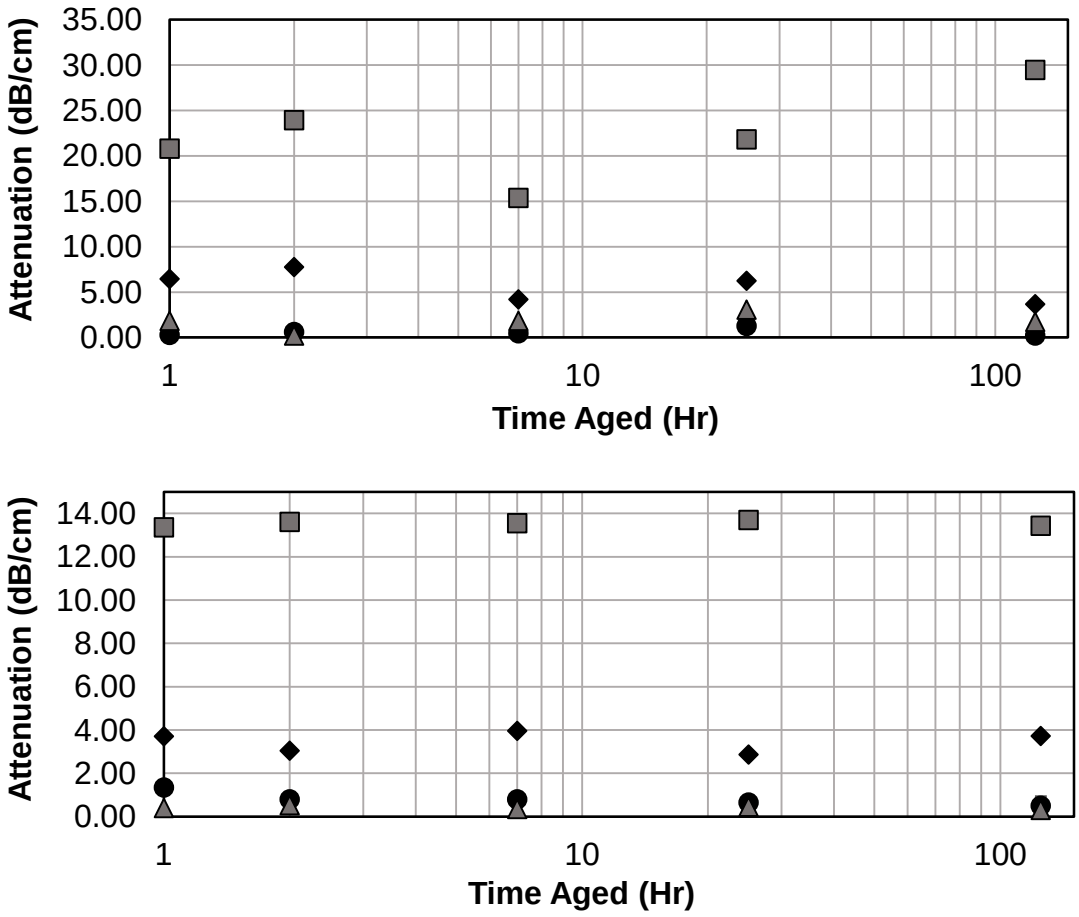

***Figure A-2**: Change in attenuation values for resin Grades 1, 2, 4, and 6 after exposure to either Toluene (**Top**), 10% Igepal (**Middle**) or B100 Biodiesel (**Bottom**) after select periods of time.* ● = Grade 1, ■ = Grade 2, ▲ = Grade 4, and ◆ = Grade 6.

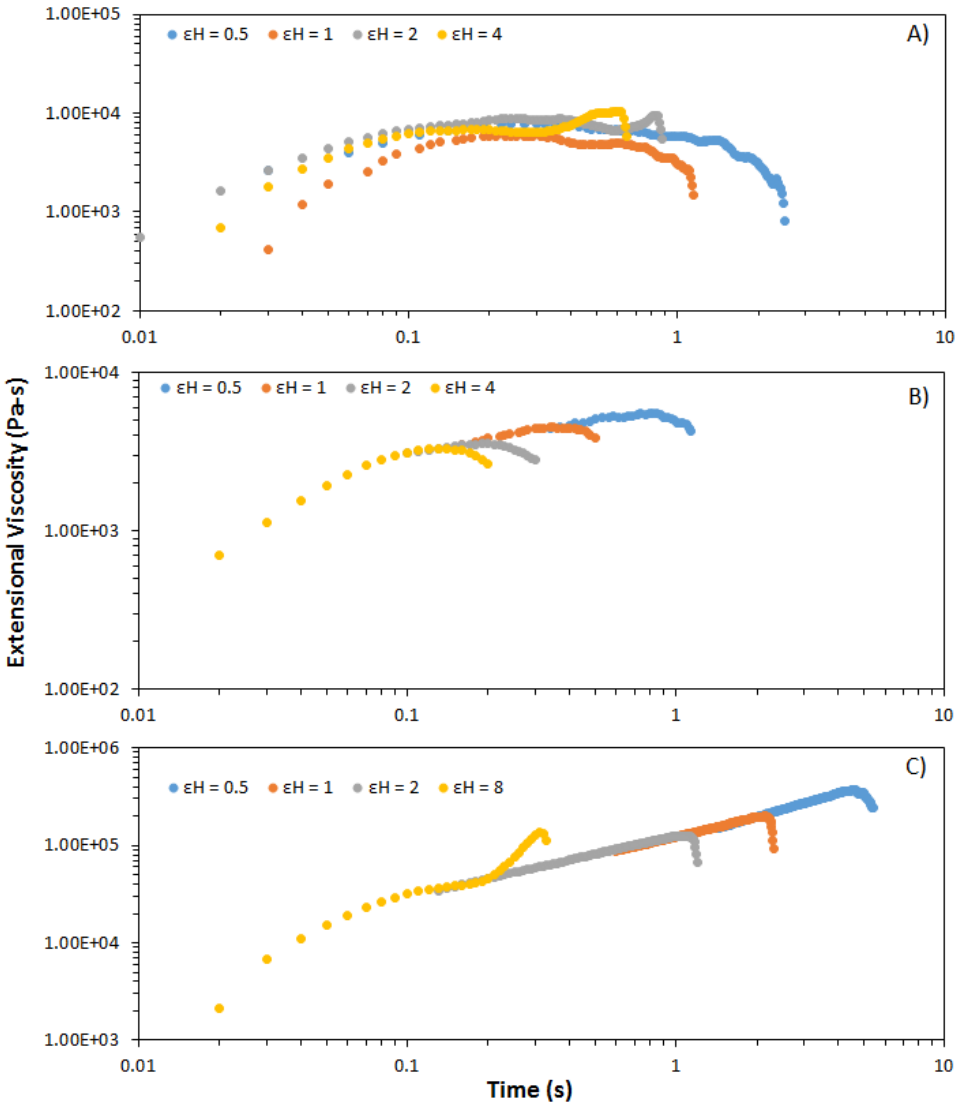

***Figure A-3**: Extension viscosity curves for Grade 1 (A), Grade 2 (B) and Grade 4 (C) polymer.*

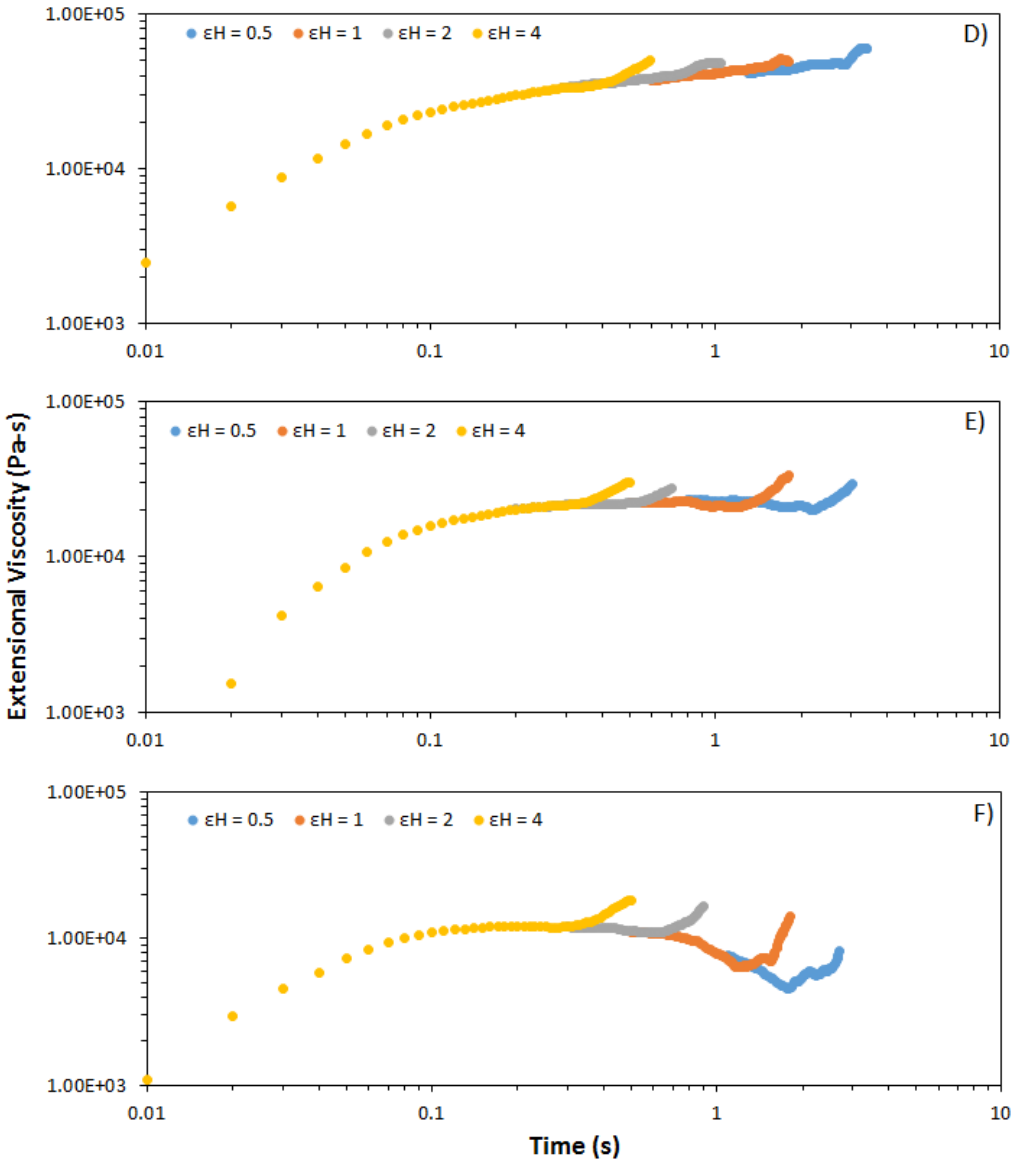

***Figure A-4**: Figure A-3: Extension viscosity curves for Grade 5 (D), Grade 6 (E) and Grade 7 (F) polymer.*

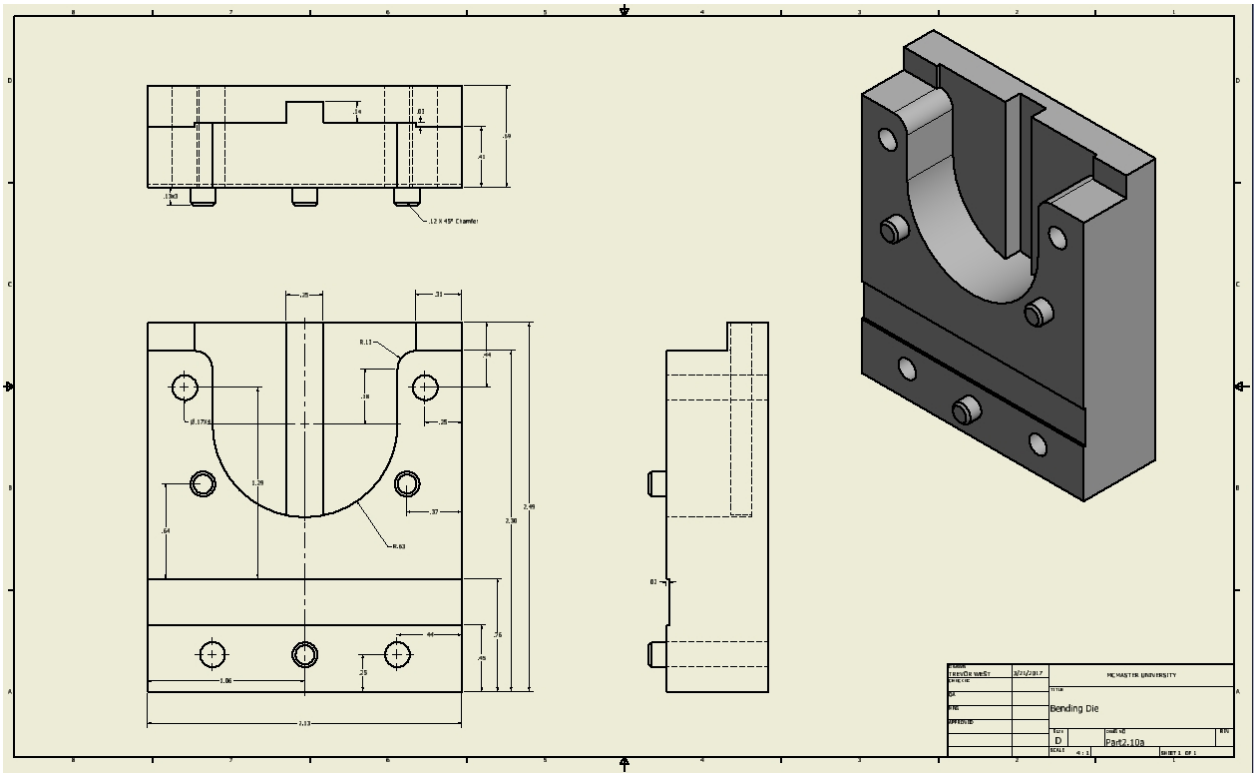

***Figure A-5**: Engineering drawing of one half of the split bending die used for sample creation in the force profiling ESCR test.*

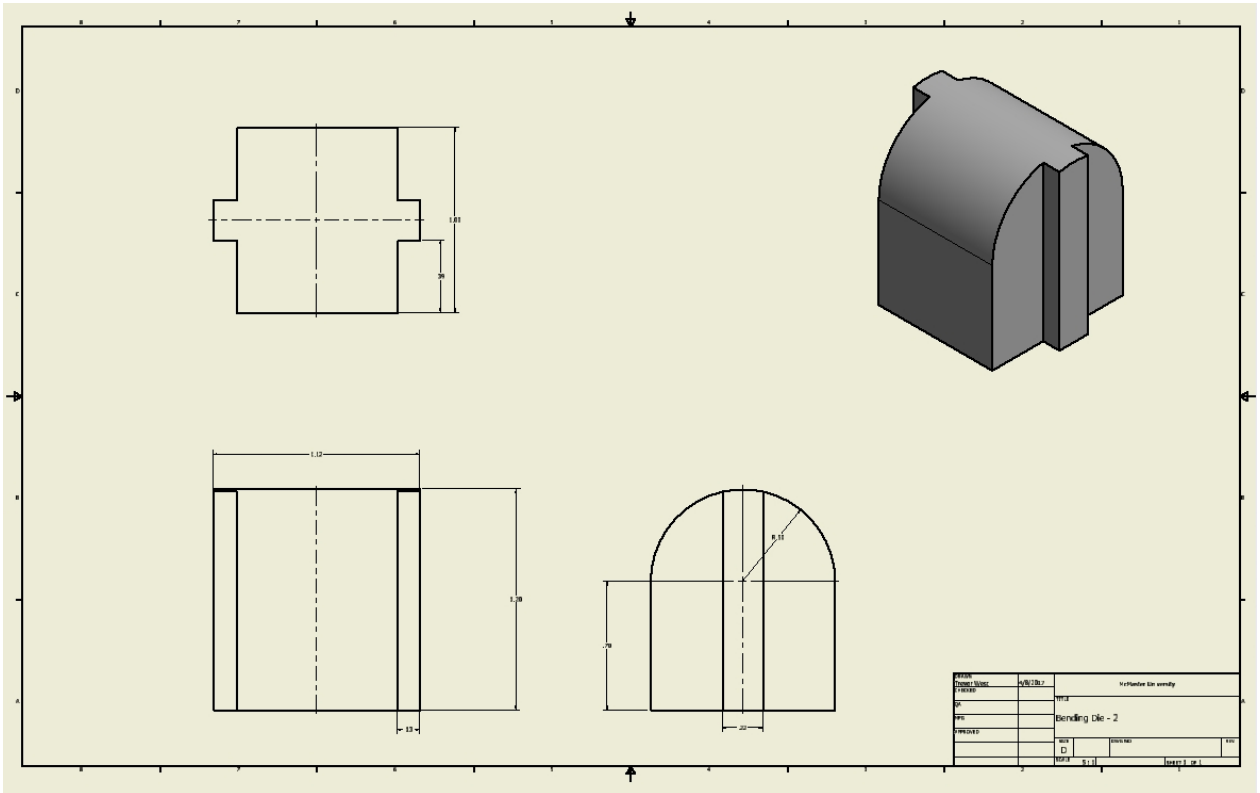

***Figure A-6**: Engineering drawing of the male plunger used in sample creation in the force profiling ESCR test.*